Food Hydrocolloids 137 (2023) 108299

Contents lists available at ScienceDirect

Food Hydrocolloids

journal homepage: www.elsevier.com/locate/foodhyd

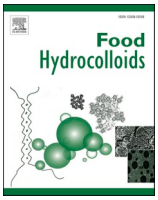

Targeted hydrolysis of native potato protein: A novel workflow for obtaining hydrolysates with improved interfacial properties

Simon Gregersen Echers [a,1,*], Ali Jafarpour [b,1], Betül Yesiltas [b], Pedro J. García-Moreno [b,c], Mathias Greve-Poulsen [d], Dennis K. Hansen [e], Charlotte Jacobsen [b], Michael Toft Overgaard [a], Egon Bech Hansen [f]

[a] Section for Biotechnology, Department of Chemistry and Bioscience, Aalborg University, Frederik Bajers Vej 7H, 9220, Aalborg, Denmark
[b] Research Group for Bioactives - Analysis and Application, National Food Institute, Technical University of Denmark, Kemitorvet, 201, Kgs Lyngby, 2800, Denmark
[c] Department of Chemical Engineering, University of Granada, Av. de Fuente Nueva, s/n, 18071, Spain
[d] KMC AmbA, Herningvej, 60, Brande, 7330, Denmark
[e] Lihme Protein Solutions A/S, Brydehusvej 30L, Ballerup, 2750, Denmark
[f] Research Group for Gut, Microbes and Health, National Food Institute, Technical University of Denmark, Kemitorvet, 202, 1250, Kgs Lyngby, 2800, Denmark

ARTICLE INFO

Keywords:
Potato protein
Targeted hydrolysis
Peptide emulsifiers
Interfacial properties
Quantitative proteomics
Peptide identification

ABSTRACT

Peptides and protein hydrolysates are promising alternatives to substitute chemical additives as functional food ingredients. In this study, we present a novel workflow for producing a potato protein hydrolysate with improved emulsifying and foaming properties using quantitative proteomics and bioinformatic prediction to facilitate targeted hydrolysis design. Based on previous studies, we selected 15 potent emulsifier peptides derived from abundant potato proteins as targets. Through *in silico* analysis, we determined that from a range of industrial proteases (Neutrase (Neut), Alcalase (Alc), Flavourzyme (Flav) and Trypsin (Tryp)), Tryp was found more likely to release peptides resembling the targets. After applying all proteases individually, hydrolysates were assayed for *in vitro* emulsifying and foaming properties. No direct correlation between degree of hydrolysis and interfacial properties was found. Tryp (E/S = 3%) produced a hydrolysate (DH = 5.4%) with high aqueous solubility and the highest ($P < 0.05$) emulsifying and foaming abilities, validating the hypothesis. Using LC-MS/MS, we identified >10,000 peptides in each hydrolysate. Peptide mapping revealed that random overlapping with known peptide emulsifiers is not sufficient to quantitatively describe hydrolysate functionality. However, validated release of targeted peptides by 3% Tryp appears to increase surface activity of the hydrolysate. Our data also suggest that terminal hydrophobic anchor domains may be important for high interfacial partitioning and activity. While modest yields and residual unhydrolyzed protein indicate room for process improvement, this work shows that bioinformatics-guided and data-driven targeted hydrolysis is a promising, interdisciplinary approach to facilitate process design for production of functional hydrolysates from alternative protein sources.

1. Introduction

Potato (*Solanum tuberosum*) is the fourth most cultivated crop with a global production of about 370 million tonnes in 2018 (Food and Agriculture Organization of the United Nations, 2020). Potatoes are the second highest protein providing crop per area grown after wheat, and despite a modest protein content of 1–2% depending on cultivar (Camire, Kubow, & Donnelly, 2009; Jørgensen, Stensballe, & Welinder, 2011; Van Koningsveld et al., 2006), they are still regarded as a highly attractive source of food protein due to both high nutritional quality and functional properties (Waglay & Karboune, 2016b). Potato proteins are often classified according to their cellular function with patatin, also known as tuberin, as the major fraction. Patatins are highly homologous storage proteins with molecular weights (MWs) from 40 to 45 kDa and

* Corresponding author.
E-mail addresses: sgr@bio.aau.dk (S. Gregersen Echers), alijaf@food.dtu.dk (A. Jafarpour), betye@food.dtu.dk (B. Yesiltas), pjgarcia@ugr.es (P.J. García-Moreno), mgp@kmc.dk (M. Greve-Poulsen), d.hansen@lps-dk.com (D.K. Hansen), chja@food.dtu.dk (C. Jacobsen), mto@bio.aau.dk (M.T. Overgaard), egbh@food.dtu.dk (E.B. Hansen).
[1] Simon Gregersen Echers and Ali Jafarpour contributed equally to this work.

https://doi.org/10.1016/j.foodhyd.2022.108299
Received 30 May 2022; Received in revised form 20 October 2022; Accepted 7 November 2022
Available online 10 November 2022

pIs in the range of 4.8–5.2 (Kärenlampi & White, 2009), which constitute 35–40% of the tuber protein depending on the specific cultivar (Løkra & Strætkvern, 2009). Likewise, protease inhibitors constitute 30–40% of the total tuber protein (Bauw et al., 2006; Jørgensen, Bauw, & Welinder, 2006), but represent a group of more diverse proteins with MWs from 5 to 25 kDa (Heibges, Glaczinski, Ballvora, Salamini, & Gebhardt, 2003; Pouvreau et al., 2001) which can be divided into sub-groups based on sequence homology and thus targets for inhibition (García-Moreno, Gregersen, et al., 2020; Heibges et al., 2003).

Directly isolated from potato fruit juice (PFJ), native potato protein has been reported to exhibit high solubility as well as foaming and emulsifying activity, which has primarily been ascribed to the high patatin content (Ralet & Guéguen, 2000; Schmidt et al., 2019; Van Koningsveld et al., 2001, 2006). To achieve these desirable characteristics, it is important to use appropriate extraction methods to maintain the proteins in their native and intact form, which, from the industrial point of view, would be costly. Thus, the industrially isolated potato protein, mainly obtained in denatured form through rather harsh heat coagulation and acid precipitation, lacks those above-mentioned functionalities. However, due to high content of amino acids with hydrophobic functional groups, in particular, with branched (isoleucine, leucine, and valine) and aromatic (phenylalanine and tyrosine) side chains (Refstie & Tiekstra, 2003), techno-functionality of potato protein can potentially be improved when the large, denatured proteins undergo a specific set of hydrolysis steps to yield smaller peptides (Aluko, 2018; Li-Chan, 2015; Moreno, Cuadrado, Marquez Moreno, & Fernandez Cuadrado, 1993; Rodan, Fields, & Falla, 2013; Wang & Xiong, 2005). Enzymatically released peptides may display better functional properties than their parent protein molecules and consequently exhibit higher activity in food systems (Kamnerdpetch, Weiss, Kasper, & Scheper, 2007; Moreno et al., 1993). This substantiates why protein hydrolysates are receiving increased attention to replace chemical additives in foods and have already found their way to market in various applications (Ashaolu, 2020; Y.-H. Wu, Samuel, Chen, Wu, & Chen, 2022). Moreover, potato protein hydrolysates have also been shown to have beneficial health effects *in vivo* (Chuang et al., 2020), illustrating their potential as both a functional and bioactive ingredients.

Amphiphilic surfactants are widely used as emulsifiers as they contain both hydrophobic and hydrophilic regions, capable of reorganising at the oil-water interface and thereby stabilize emulsions by decreasing interfacial tension between two immiscible liquids (McClements & Jafari, 2018). In this respect, the use of peptides as natural emulsifiers and biosurfactants has received increasing attention over the past few decades from both the academic and the industrial sector (Adjonu, Doran, Torley, & Agboola, 2014; Dexter & Middelberg, 2008; Hanley & James, 2018; Le Guenic, Chaveriat, Lequart, Joly, & Martin, 2019). Peptides are complex polymer chains combining (at least) twenty different amino acid monomers with different physico-chemical properties and thus, the combinatorial space is tremendous and scales by peptide length, n, as (at least) 20^n. Although the specific mechanisms and prerequisites for potent peptide emulsifiers still remains only superficially characterized, our understanding of the underlying molecular properties continue to expand (Ricardo, Pradilla, Cruz, & Alvarez, 2021). Recent work has investigated the influence of factors such as interfacial peptide structure (Dexter, 2010; Du et al., 2020; García--Moreno et al., 2021; Lacou, Léonil, & Gagnaire, 2016), physico-chemical properties such as length and charge (García-Moreno, Gregersen, et al., 2020; Lacou et al., 2016; Liang et al., 2020; Yesiltas et al., 2021), amino acid composition (Enser, Bloomberg, Brock, & Clark, 1990; Saito, Ogasawara, Chikuni, & Shimizu, 1995; Siebert, 2001), and specific sequence patterns (Jafarpour, Gregersen, et al., 2020; Mondal et al., 2017; Nakai et al., 2004; Wychowaniec et al., 2020). Although various factors do appear to influence emulsification, the potential appears to indeed depend significantly on the propensity of a given peptide to adopt a more well-defined amphiphilic structure at the interface (Dexter & Middelberg, 2008; Enser et al., 1990; Saito et al., 1995). This property, in turn, is governed by these underlying factors. While not appearing to be governed by the exact same molecular mechanisms, the stabilization of the air-water interface in foams has been suggested to also depend on peptide amphiphilicity (Enser et al., 1990; Jafarpour, Gregersen, et al., 2020).

Consequently, identification and molecular characterization of isolated peptides could enhance the understanding of functional mechanism and potential of enzymatic protein hydrolysates in food systems, such as emulsions and foams. Moreover, it would allow for development of targeted processes for release of specific peptides with known functional properties. This, in turn, could result in improved modification of a potato by-product to generate more value added ingredients with beneficial properties (Karami & Akbari-adergani, 2019). Waglay and Karboune (2016a) characterized the structure of enzymatically generated peptides from potato protein, however, these authors did not correlate the specified characterization with functionality properties (Waglay & Karboune, 2016a). García-Moreno, Jacobsen, et al. (2020) investigated the emulsifying activity of six potato peptides (23–29 amino acids) predicted by bioinformatics as having potentially different predominant structure at the oil/water interface (e.g. α-helix, β-strand or unordered). The authors found that γ-peptides (half-hydrophobic and half-hydrophilic peptides with axial amphiphilicity), showed higher emulsifying activity, compared to α-helix and β-strand peptides, in agreement with their predictions . However, generalization is not possible on such limited data. The study was followed by a more elaborate investigation of potato protein derived emulsifier peptides (García-Moreno, Gregersen, et al., 2020), showing that this could indeed not be generalized. In fact, the most promising peptide emulsifier (γ1) was later shown to adopt a predominantly α-helical conformation at the interface, thereby possessing both axial and facial amphiphilicity (García-Moreno et al., 2021). Although the structure-function relationship of emulsifier peptides is more complex than predictable secondary structure and amphiphilicity, the two factors can be regarded as good indicators of emulsification potential (Saito et al., 1995).

Until now, most studies on protein hydrolysates have been conducted using a trial-and error approach, where various industrial proteases were used to digest proteins in an untargeted manner. In such studies, process parameters (e.g. protease selection, pH, temperature, protein concentration, enzyme/substrate ratio, and time) were usually optimised in respect to bulk hydrolysate characteristics such as yield or functionality, with little or no attention to peptide-level insight. The application of mass spectrometry has in these instances mainly been focused on identification of peptides with high intensities in the bulk hydrolysate or in the high activity fractions. While such analysis may provide insight on peptides potentially responsible for the observed bulk functionality, it does not provide sufficient evidence unless functional properties are validated for the isolated peptide. In this study, we present the fundamentally different approach of bioinformatics-guided and data-driven process design for targeted hydrolysis. Building on existing knowledge on potato protein-derived peptide emulsifiers, we present a workflow where *in silico* sequence analysis is used as a guide for protease selection. By prediction of peptide release based on protease specificity, we hypothesize that application of specific proteases should produce a hydrolysate with better surface active (i.e. emulsifying and potentially foaming) properties. The targeted hydrolysis design is benchmarked against a range of commonly used industrial proteases, and the hydrolysates are characterised for their bulk physico-chemical and functional properties with particular focus on emulsification of fish oil and foam formation. Ultimately, we apply mass spectrometry-based proteomics analysis to qualitatively and quantitatively characterize the peptidome of the hydrolysates and relate these findings to both *in vitro* functionalities, predicted peptide release, and *a priori* knowledge on potato peptide emulsifiers. With this approach, we showcase how proteomics and bioinformatics may lay the basis for targeted process design in the future of peptide-based functional food ingredient development and production.

2. Materials and methods

Potato protein isolate (PPI) (87% protein, determined by Kjeldal-N and Dumas) was supplied by KMC AmbA (Brande, Denmark). The PPI was obtained using a proprietary, cold extraction method yielding native, non-denatured proteins. Alcalase (Alc) 2.4L (2.4 AU/g), Neutrase (Neu) 0.8L (0.8 AU/g), Flavourzyme (Flav) 1000 L (1000 LAPU/g), and Trypsin (Tryp) (Pancreatic Trypsin Novo (PTN) 6.0S (6.0 AU/g) were provided by Novozymes A/S, (Bagsværd, Denmark). Distilled deionized water was used for the preparation of all solutions during hydrolysate production. As references for emulsification experiments, sodium caseinate (SC) and purified, native patatin were used. SC (Miprodan 30) was supplied by Arla Foods Ingredients AmbA (Viby J, Denmark) and patatin was purified from the PPI by Lihme Protein Solutions (Kongens Lyngby, Denmark) using a gentle, sequential precipitation through a proprietary pH-shift methodology. All chemicals used were of analytical grade.

2.1. Target peptide selection and in silico sequence analysis

Previously investigated peptides derived from potato proteins were evaluated for emulsification potential based on published data (García-Moreno et al., 2021; García-Moreno, Gregersen, et al., 2020; García-Moreno, Jacobsen, et al., 2020; Yesiltas et al., 2021). Peptides were categorized (Table A.1) on a three-level scale (high (1), intermediate (2), and low (3)) according to their ability to i) reduce oil/water interfacial tension (IFT), ii) decrease oil droplet size, and iii) lead to physically stable emulsions during storage in comparison to SC (see supplementary for further descriptions of criteria). Peptides classified as high or intermediate in all three categories were selected for further *in silico* sequence analysis and ranked by their mean score across the three categories (and different studies, where applicable).

To investigate potential release by enzymatic hydrolysis using the available proteases, the specific peptide was localized in the protein of origin (according to the original study) and the region of the protein containing the peptide and 15 amino acids up- and downstream (Table 1) extracted from Uniprot (Consortium et al., 2021). Cleavage specificity of the proteases was used to manually analyze potential hydrolysis of the protein region, where Tryp specificity is well-established and cleaves after Lys/Arg (K/R). Alc and Neut are broad specificity proteases, but supplier specificity (Novozymes A/S) was used for *in* silico analysis. As such, Alc has a strong preference to cleave after Leu/-Phe/Tyr/Gln (L/F/Y/Q), while Neut shows preference to cleave before Leu/Ile/Phe/Val (L/I/F/V). Flav is a complex mixture of endo- and exoproteases (Rabe et al., 2015), and cleavage specificity has not been established. As such, Flav was used merely as a reference protease due to its widespread use in the food industry.

2.2. Potato protein hydrolysate preparation

Potato protein hydrolysates (PPHs) were produced from a native PPI, using two enzymatic hydrolysis strategies; (A) free-fall pH hydrolysis of native PPI, and (B) free-fall pH mode with protein heat denaturation prior to hydrolysis. In method A, a 1% (w/v) protein solution was prepared by gradual addition of PPI to distilled water and solubilized for 15 min by magnetic stirring. In method B, a 10% (w/v) PPI solution was prepared, heated to 90 °C for 30 min, and resulting slurry was diluted 1:1 with distilled water to a final protein concentration of 4.35% (w/v). The pH of all PPI solutions was adjusted to 8.0 by 1M NaOH followed by addition of individual proteases (Alc, Neut, Flav, or Tryp) at varying enzyme/substrate (E/S) ratio. For method A, E/S ratios of 0.1%, 0.5%, and 1% were applied while for method B, E/S ratios of 0.1% 1%, and 3% were applied. In both methods, hydrolysis was carried out at 50 °C for 2 h. pH and temperature were selected to accommodate activity ranges of

Table 1
Cluster representation of final target peptides. Peptides are annotated in accordance with the reference study (Ref) and listed along with the Uniprot identifier (AC#), protein name, sequence window (target peptide **(in bold)** along with the N- and C-terminal 15 amino acids cleavage window for *in silico* sequence and release analysis), average score (see Table A1), and the cluster number (based on sequence overlap in identical or isoform proteins). Below each cluster, the aligned cluster consensus sequence is indicated with variable residues depicted as *"X"*.

Pep	AC#	Protein	Sequence window	Score	Ref.*	Cluster
γ1	P15477	Patatin-B2	AKLEEMVTVLSIDGG**GIKGIIPAIILEFLEGQLQEVDNNKDAR**LADYFDVIGGTSTGG	1.0	a,b,d	
γ104	Q3YJT3	Pat-2-Kuras 1	GEMVTVLSIDGGGIK**GIIPATILEFLEGQLQEVDNNKDAR**LADYFDVIGGTSTGG	1.0	c	
γ105	Q3YJT4	Pat-1-Kuras 2	EEMVTVLSIDGGGIK**GIIPGTILEFLEGQLQK**MDNNADARLADYFDV	1.0	c	
γ48	Q3YJT3	Pat-2-Kuras 1	GEMVTVLSIDGGGIK**GIIPATILEFLEGQLQEVDNN**KDARLADYFDVIGGT	1.3	b	1
γ75	P15477	Patatin-B2	EEMVTVLSIDGGGIK**GIIPAIILEFLEGQLQEVDNNKDAR**LADYFDVIGGTSTGG	1.3	d	
γ76	P15477	Patatin-B2	EEMVTVLSIDGGGIK**GIIPAIILEFLEGQLQEVDNNK**DARLADYFDVIGGTS	1.3	d	
	Consensus		GIKGIIP*XX*ILEFLEGQLQ*X*VDNNKDAR			
γ40	Q3S474	KTI-B	NLLYCPVTSTMICPF**SSDDQFCLKVGVV**HQNGKRRLALVKDNP	1.2	b,d	
β22	Q3S474	KTI-B	LGYNLLYCPVTSTMI**CPFSSDDQFCLKVGV**VHQNGKRRLALVKDN	1.8	b,d	2
	Consensus		CPFSSDDQFCLKVGVV			
α12	P15477	Patatin-B2	LVQVGETLLKKPVSK**DSPETYEEALKRFAKLLSD**RKKLRANKASH**	1.3	b,d	
α10	P15477	Patatin-B2	EANMELLVQVGETLL**KKPVSKDSPETYEEALKRFAKLLSDRKKL**RANKASH**	1.7	b,d	3
	Consensus		KKPVSKDSPETYEEALKRFAKLLSDRKKL			
γ36	Q3YJT3	Pat-2-Kuras 1	LQEVDNNKDARLADY**FDVIGGTSTGGLLTAMITTPNENNRP**FAAAKDIVPFYFEHG	1.3	b,d	4
	Consensus		FDVIGGTSTGGLLTAMITTPNENNRP			
β27	Q3S488	KTI-A	VRFIPLSTNIFEDQL**LNIQFNIPTPKLC**VSYTIWKVGNINAPLR	1.5	b,d	5
	Consensus		LNIQFNIPTPKLC			
γ38	Q3S474	KTI-B	PVTSTMICPFSSDDQ**FCLKVGVVHQNGKRRLALVKDNP**LDVSFKQVQ**	1.7	b,d	
γ49	Q3S477	KTI-B	YCPATMICPFCSDDE**FCLKVGVIHQNGKRRLALVK**DNPLDVSFKQVQ**	2.0	b	6
	Consensus		FCLKVGV*X*HQNGKRRLALVKDNP			
α2	P15477	Patatin-B2	DICYSTAAAPIYFPP**HHFVTHTSNGARYEFNLVDGAVATVGDPA**LLSLSVATRLAQEDP	2.0	a	7
	Consensus		HHFVTHTSNGARYEFNLVDGAVATVGDPA			

* References: a (García-Moreno, Jacobsen, et al., 2020), b (García-Moreno, Gregersen, et al., 2020), c (Yesiltas et al., 2021), and d (García-Moreno et al., 2021).
** End of protein sequence.

all proteases according to manufacturer (Novozymes A/S supplied information).

Following hydrolysis, the pH of the solution was adjusted to 7.0 with either 1M NaOH or 1M HCl and supernatants were heated to 90 °C for 15 min for enzyme inactivation. After cooling by tap water, solutions were centrifuged at 10,000×*g* for 20 min at 20 °C and the supernatant collected. The PPH was lyophilized and stored at 4 °C until further analysis. The two applied hydrolysis strategies are illustrated in Fig. 1.

2.3. Hydrolysis evaluation

To evaluate the different process designs, degree of hydrolysis (DH), nitrogen recovery (NR), crude protein (CP), and yield (by mass balance) were determined for each individual process.

DH was determined based on α-amino nitrogen content as previously described (Jafarpour, Gregersen, et al., 2020) with minor modifications, adjusting for the α-amino nitrogen content of the untreated substrate. Briefly, free α-amino content of PPHs was determined using the PFAN-25 free amino nitrogen assay kit (PractiChrom, USA) measured using A_{530} on a Picoexplorer (USHIO INC, USA), according to manufacturer guidelines, using glycine as reference for standard curve generation. DH was calculated as:

$$DH\% = \frac{AN_i - AN_0}{AN_{tot} - AN_0} \times 100$$

where AN_i is the concentration of α-amino nitrogen (mM/g substrate) resulting from hydrolysis at a given time, i, AN_0 is the α-amino nitrogen content of the untreated substrate, and AN_{tot} is the total amount of α-amino nitrogen content following complete hydrolysis with 6 M HCl at 110 °C for 24 h, as previously described (Jafarpour, Gomes, et al., 2020). AN_{tot} was based on duplicate amino acid (AA) analysis. All measurements were performed in triplicates.

The average peptide chain length (PCL_{DH}) was calculated as:

$$PCL_{DH} = \frac{1}{DH(\%)} * 100$$

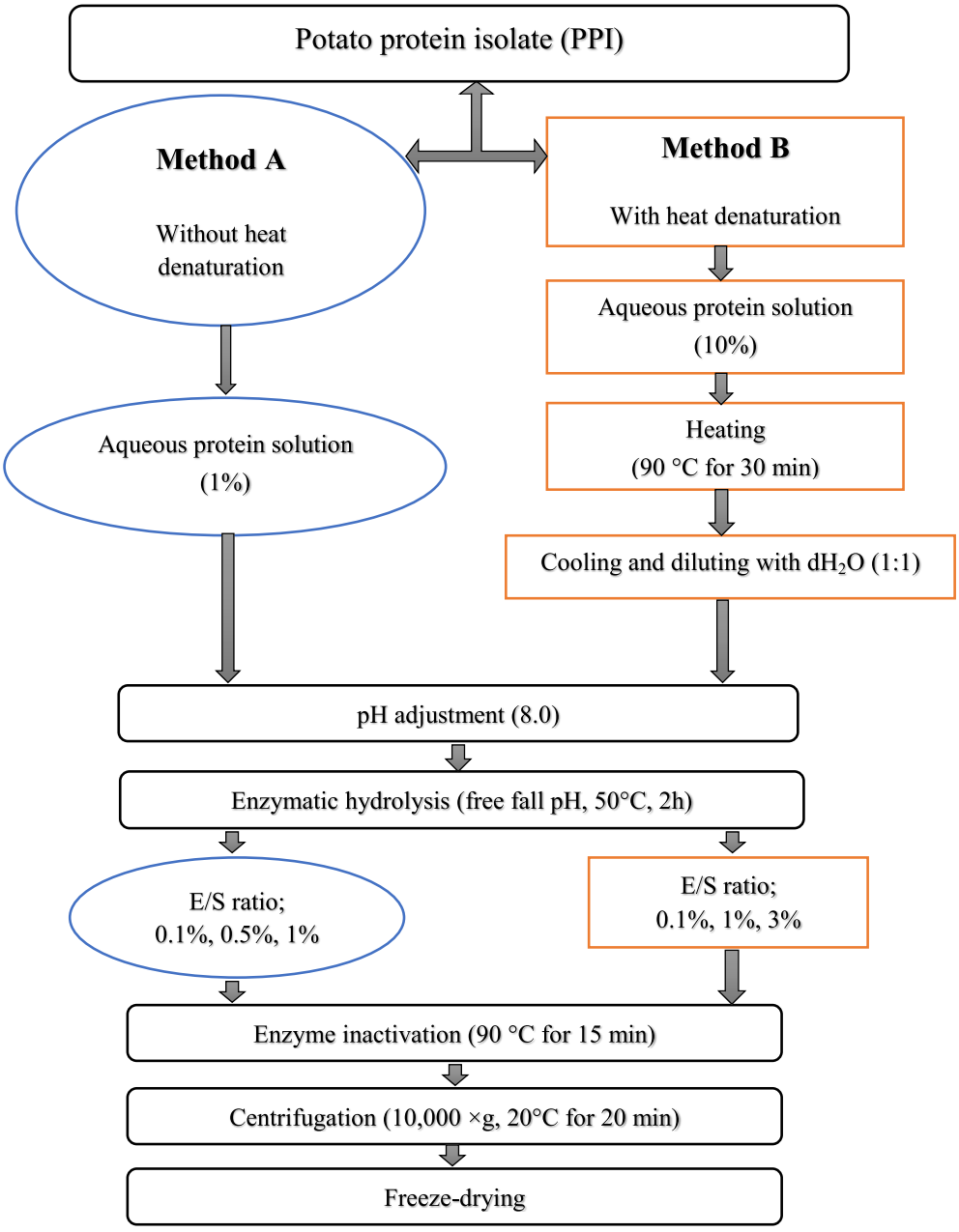

Fig. 1. Flow chart for the enzymatic hydrolysis of potato protein isolate (PPI) by application of Alc, Neut, Flav or Tryp. The two different approaches are illustrated, where the left process (Method A) was performed without initial heat denaturation of PPI while the right process (Method B) included heat denaturation to inactivate protease inhibitors. Steps specific for method A are depicted in circles while steps specific for method B are depicted in squares. Common steps are depicted as rounded squares spanning both workflows.

Total nitrogen was determined using the Dumas combustion method using a fully automated Rapid MAX N (Elementar Analysensysteme GmbH, Langenselbold, Germany), and NR in the soluble fraction was determined as previously reported:

$$NR\ (\%) = \frac{N_{PPH} \times m_{PPH}}{N_i \times m_i} \times 100\%$$

where N_{PPH} is nitrogen content (%) in the PPH, m_{PPH} is the mass (g) of analyzed PPH, N_i is the nitrogen content (%) of the initial substrate, and m_i is the mass (g) of the initial substrate analyzed. Prior to analysis, the system was calibrated using multiple blanks, aspartic acid, and wheat protein isolates. The CP was estimated using a standard industrial nitrogen to protein conversion factor of 6.25 (Jones, 1931; Mariotti, Tomé, & Mirand, 2008).

The yield of hydrolysis was determined as the mass ratio to the initial substrate mass, as

$$Yield\ (\%) = \frac{m_{PPH}}{m_i} \times 100\%$$

where m_{PPH} is the mass (g) of obtained PPH after lyophilization and m_i is the mass (g) of initial substrate.

2.4. Bulk characterization of hydrolysates

All hydrolysates were characterized for basic physicochemical properties in bulk, including relative solubility, bulk density, color, and compositional visualization by SDS-PAGE.

The relative solubility of PPI/PPHs at 10 mg/mL was determined based on nitrogen content by Dumas. Briefly, 200 mg PPH was dissolved in 20 mL of 0.1 M sodium phosphate buffer (pH = 7.4), vortexed for 10 s, shaken at 80 rpm for 30 min, and centrifuged at 7500×*g* for 15 min. PPH solubility was calculated as:

$$Solubility\ (\%) = \frac{P_{sup}}{P_{tot}} \times 100\%$$

where P_{sup} is protein/peptide content in supernatant and P_{tot} is total protein/peptide content in PPI the respective PPH as obtained for determination of NR. Measurements were performed in triplicate.

The bulk density of the PPHs was determined according to (Jafarpour, Gomes, et al., 2020). Briefly, 5g PPH was added to a 50 mL graduated cylinders and gently tapped 10 times on the lab bench. Bulk density was reported as g/mL.

The tristimulus color parameters ($L^*a^*b^*$) of PPHs were recorded using a Miniscan XE colorimeter (Hunter Lab, Reston, Virginia, USA) and the whiteness of PPHs was determined in accordance with (Hashemi & Jafarpour, 2016) and calculated as:

$$W = 100 - \sqrt[2]{(100 - L^*)^2 + a^{*2} + b^{*2}}$$

where, W is whiteness index, L^*; indicating lightness from black (0) to white (100); a^*; indicating redness from green (- 120) to red (+120); and b^*; indicating yellowness going from blue (−120) to yellow (+120). Measurements were performed in triplicate.

To visualize the extent of hydrolysis, PPHs were analyzed by SDS-PAGE. using SurePAGE 4–20% gradient Bis-Tris gels (Genscript, Picastaway, NJ, USA) under reducing conditions, as previously described (Jafarpour, Gregersen, et al., 2020). As controls, the unhydrolyzed PPI sample and a process control (PPI with no added protease but same treatment) were included.

2.5. Characterization of basic interfacial properties

Interfacial properties of hydrolysates were evaluated by determination of emulsifying activity index (EAI), emulsion stability index (ESI), foaming capacity (FC), and foaming stability (FS).

EAI and ESI were determined using the method described by (Pearce & Kinsella, 1978) with slight modifications, as previously described (Jafarpour, Gregersen, et al., 2020). Briefly, 15 mL PPH in distilled water (2 mg/mL) was mixed with 5 mL rapeseed oil by an ultraturax homogenizer (IKA, Germany) at speed of 9,500 rpm for 60 s without pH adjustment. Fifty μL aliquots were pipetted from the bottom of the container at 0 and 10 min after homogenization and added to 5 mL of 0.1% sodium dodecyl sulfate (SDS) solution and mixed by gentle shaking. The absorbance of the diluted solution was measured at 500 nm using a spectrophotometer (SHIMADSU UV-1280, Japan). EAI was calculated as:

$$EAI\left(\frac{m^2}{g}\right) = \frac{2 \times 2.303 \times A_0 \times D}{\varnothing \times c \times 10,000}$$

where A_0 is the absorbance at 500 nm immediately following homogenization, D is dilution factor (100), $\varnothing$ is oil volume fraction (0.25) and c is protein concentration (g/mL).

2.6. ESI was calculated as

$$ESI(min) = \frac{A_0 \times \Delta T}{\Delta A}$$

where ΔT is equal to 10 min and ΔA is the difference in absorbance at 500 nm after 0 and 10 min ($\Delta A = A_0\text{-}A_{10}$). Enriched patatin, untreated PPI, and SC solutions (2 mg/mL) were used as references. Measurements were performed in triplicates.

FC and FS were determined according to the method by (Elavarasan, Naveen Kumar, & Shamasundar, 2014). Accordingly, 0.1% (w/v) PPH in distilled water was homogenized at 9,500 rpm for 120 s using an Ultraturrax (IKA, Germany), and poured into a 200 mL graduated cylinder. FC was calculated as:

$$FC(\%) = \frac{V^0_{foam}}{V_{init}} \times 100\%$$

where V^0_{foam} is the foam volume immediately after homogenization and V_{init} is the initial sample volume.

FS was determined after a 30 min resting period (FS_{30}) and calculated as:

$$FS_{30}(\%) = \frac{V^{30}_{foam}}{V^0_{foam}} \times 100\%$$

where V^{30}_{foam} is the foam volume after 30 min. Measurements were performed in triplicates.

2.7. Peptidomic analysis by LC-MS/MS

Lyophilized PPH was solubilized in a detergent-containing buffer, reduced and alkylated in-solution, and desalted using C-18 StageTips, and dried by SpeedVac, as previously described (Jafarpour, Gomes, et al., 2020). Desalted peptides were solubilized in solvent A (0.1% aq. formic acid (FA)) and 1 μg (determined by NanoDrop (Thermo Scientific Bremen, Germany)) was loaded and separated on an EASY-nLC (Thermo Scientific) equipped with a reverse phase (RP) Acclaim Pepmap Nanotrap column (C18, 100 Å, 100 μm × 2 cm, nanoViper fittings (Thermo Scientific)) followed by a RP Acclaim Pepmap RSLC analytical column (C18, 100 Å, 75 μm × 50 cm, nanoViper fittings (Thermo Scientific). Eluted peptides were introduced into a Q Exactive HF mass spectrometer (Thermo Scientific) via a Nanospray Flex ion source (Thermo Scientific) using a fused silica needle emitter (New Objective, Woburn, MA, USA). Samples were loaded at 8 μL/min and eluted by constant flow at 300 nL/min during a 120 min ramped gradient, ranging from 5 to 100% of solvent B (0.1% formic acid (FA), 80% (V/V) acetonitrile). MS data was acquired in positive mode using a Top-20 data-dependent method.

Survey scans were acquired from 200 m/z to 3,000 m/z at a resolution of 60,000 at 200 m/z and the HCD fragmentation spectra were acquired at a resolution of 30,000 at 200 m/z using an isolation window of 1.2 m/z and a dynamic exclusion window of 30 s. The maximum ion injection time was set to 150 ms for both MS and MS/MS scans. ACG target was set to 3e6 and 2e5 for MS and MS/MS scans, respectively. Charge exclusion was only applied for unassigned isotope peaks (all charge states allowed). Peptide match and exclude isotopes were enabled.

2.8. LC-MS/MS data analysis

MS raw data was analyzed in MaxQuant v.1.6.10.43 (Cox & Mann, 2008; Tyanova, Temu, & Cox, 2016), as previously described (Jafarpour, Gomes, et al., 2020). Briefly, unspecific *in silico* digestion was employed to identify peptides in the range 3–65 AAs. Data was searched against a manually curated version of the full protein database for *Solanum tuberosum* (tax:4113) from UniProt (Consortium et al., 2021) where redundant fragments were removed, as previously described (García-Moreno, Gregersen, et al., 2020). Standard settings were applied, using a 5% false discovery rate (FDR) on both peptide and protein level, including common contaminants and reverse sequences for FDR control. The mass spectrometry proteomics data have been deposited to the ProteomeXchange Consortium (http://proteomecentral.proteomexchange.org) via the PRIDE partner repository (Perez-Riverol et al., 2022) with the dataset identifier PXD034139.

Following removal of false positives and contaminants, Venn diagrams were created to visualize peptide identifications and similarity between PPHs. Peptide tables were treated according to the intensity-weighted peptide abundance estimation methodology, as previously described (Jafarpour, Gomes, et al., 2020; Jafarpour, Gregersen, et al., 2020), and average peptide length (PCL_{avg}) was calculated as:

$$PCL_{avg} = \frac{\sum_{p=1}^{n} PCL_p * I_p}{\sum_{p=1}^{n} I_p}$$

where PCL_p is the length of peptide p of n identified and quantified peptides and I_p is the MS1 intensity of the same peptide. For correlation of identified peptides with known emulsifier peptides derived from potato proteins, a set of seven selected target clusters were constructed (Table 1). For each cluster, a representative cluster sequence spanning the entire sequence with "X" representing variable residues (i.e. AAs where substitutions occur within the cluster peptides) was created. All peptides related to the class/family of proteins associated with the cluster were initially included and subjected to filtering based criteria regarding length and degree of sequence overlap (see supplementary for further information). Sequence overlap between identified peptides and a representative cluster sequence was determined through the following set of equations:

$$if\ P_E < C_S \rightarrow overlap = 0$$

$$if\ P_S > C_E \rightarrow overlap = 0$$

$$if\ P_S < C_S\ \&\ P_E \leq C_E \rightarrow overlap = \frac{1 + P_E - C_S}{L}$$

$$if\ P_S < C_S\ \&\ P_E > C_E \rightarrow overlap = \frac{1 + C_E - C_S}{L}$$

$$if\ P_S \geq C_S\ \&\ P_E \leq C_E \rightarrow overlap = 1$$

$$if\ P_S \geq C_S\ \&\ P_E > C_E \rightarrow overlap = \frac{1 + C_E - P_S}{L}$$

where P_S and P_E are the AA positions for the start and end of an identified peptide when mapped to a certain protein cluster sequence, C_S and C_E are the AA positions for the start and end of a representative cluster sequence when mapped to the same protein cluster sequence, L is the length of the identified peptide. Peptides were classified as >50%, >75%, and >95% overlap, thereby with increasing confidence of emulsifier activity with increasing sequence overlap. The five most abundant (by MS1 intensity) peptides from each PPH with >50% overlap with representative cluster sequence were extracted and mapped to the representative cluster sequence using the NCBI blastp suite. The alignment was then visualized in the NCBI multiple sequence alignment (MSA) viewer using the built-in hydropathy color scale and with substitutions indicated.

To determine the protein-level distribution of peptides in PPHs, the method of unspecific, length-normalized relative intensity, I_L^{rel}, was used (Gregersen et al., 2021, 2022). In short, the relative molar abundance of an identified protein (group) was estimated as:

$$I_{rel}^{L}(n) = \frac{I_n/L_n}{\sum_{n=1}^{p} I_n/L_n} * 100\%$$

where I_n is the intensity of protein n (i.e. sum of all peptide intensities ascribed to the protein (group)) of p quantified proteins in a given PPH and L_n is the length of protein n. Subsequently, proteins were grouped according to family/class (García-Moreno, Gregersen, et al., 2020), and the relative abundance of each class was determined.

2.9. Statistical analysis

The statistical significance between measurements was determined by variance analysis (ANOVA) using Statgraphics software (version 18.1.06 for Windows), and means were compared by Duncan's multiple comparison post-test. Statistical differences were considered to be significant at $p < 0.05$.

3. Results and discussion

3.1. In silico analysis and design of a targeted hydrolysis process

Based on previously published data on *in vitro* emulsifying properties of potato protein-derived peptides, 58 peptides were evaluated and ranked by their ability to reduce oil/water interfacial tension, mean droplet size after emulsification of 5% fish oil in water, and physical stability of the emulsion (Table A1). From the initial evaluation, 15 unique peptides with strong emulsifying properties were selected for further *in silico* analysis to identify release potential by enzymatic hydrolysis (Table 1). The 15 selected peptides group into seven clusters by sequence similarity, where particularly cluster 1, γ1-related peptides, is densely populated.

Alc has broad specificity and has been reported to cleave after a wide range of residues (Ala/Leu/Val/Phe/Tyr/Trp/Glu/Met/Ser/Lys) with varying claims throughout literature (Doucet, Otter, Gauthier, & Foegeding, 2003; Lei, Cui, Zhao, Sun-Waterhouse, & Zhao, 2014; Lu et al., 2021; Sbroggio, Montilha, Figueiredo, Georgetti, & Kurozawa, 2016). A similar lack of consensus for Neut specificity is also found in literature. Consequently, the *in silico* analysis was based on supplier specificity (Novozymes A/S, Denmark), using a 15 amino acid N- and C-terminal cleavage window, to map all cleavage sites of Alc, Neut, and Tryp (Fig. 2).

In cluster 1, a good overall compatibility with tryptic cleavage is observed. Tryp hydrolysis will result in a three AA N-terminal truncation of γ1 (resulting in γ75) and a three AA C-terminal truncation of γ75 (resulting in γ76). As the C-terminal Lys in γ76 is followed by an Asp, cleavage efficiency for Tryp may be reduced in this position (Giansanti, Tsiatsiani, Low, & Heck, 2016), making γ75 the most probable product, in line with previous studies (García-Moreno et al., 2021; García-Moreno, Gregersen, et al., 2020). While γ48, γ105, and γ106 originate from

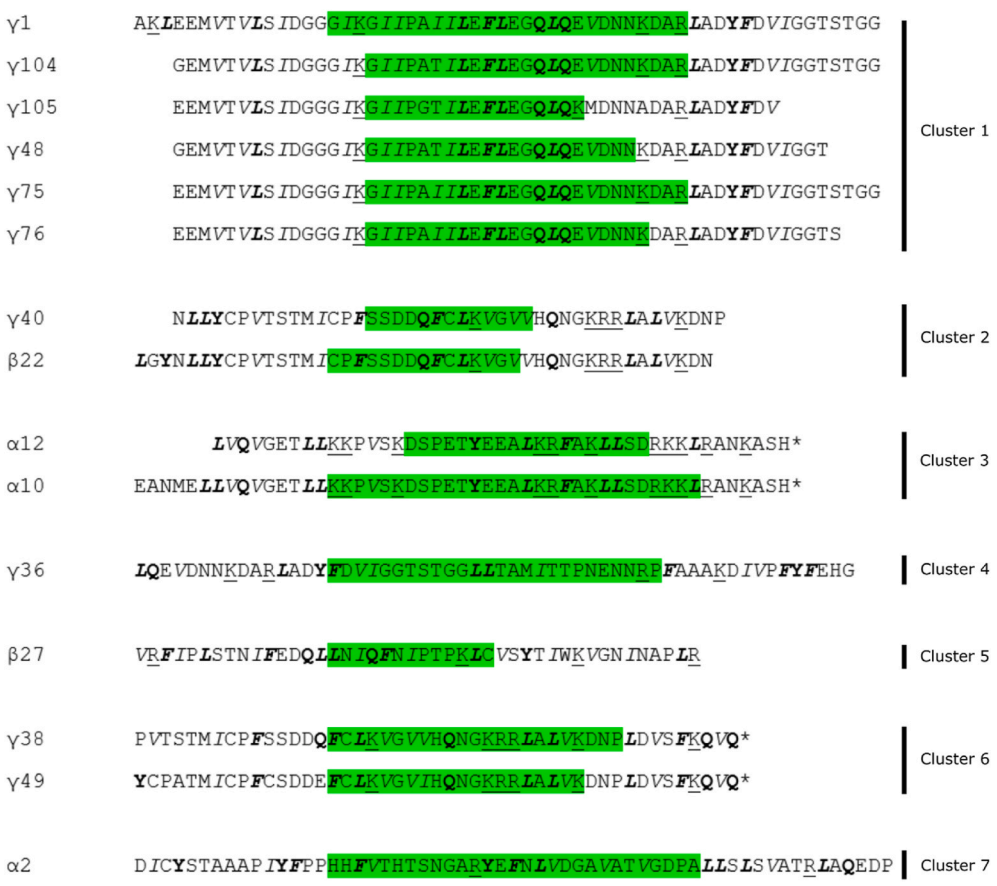

Fig. 2. Visualization of *in silico* release potential analysis for selected target peptides following enzymatic hydrolysis by Tryp, Alc, or Neut. Peptides with validated *in vitro* emulsifying properties (highlighted in green) are listed with a 15 amino acid N- and C-terminal cleavage window and clustered by sequence similarity (Table 1). Cleavage sites for Tryp (cleavage after R/K) are underlined, cleavage sites for Alc (cleavage after L/F/Y/Q) are highlighted in **bold**, and cleavage sites for Neut (cleavage before I/L/F/V) are highlighted in *italics*. Alc and Neut both cleave at Phe (F) and Leu (L). "*" indicates the end (C-terminus) of the native protein sequence. (For interpretation of the references to color in this figure legend, the reader is referred to the Web version of this article.)

other isoforms of patatin and thus contain different AA substitutions, placement of tryptic AAs is highly favourable as well. Target AAs for both Alc and Neut are abundant within all cluster 1 peptides making release of the peptides less likely. Target AAs for Neut are located favourably in both termini of cluster 1 peptides, but release of target peptides is considered unlikely in a controlled and reproducible manner.

In cluster 2, tryptic AAs are unfavourably distributed. Target AAs for both Alc and Neut are abundant in both peptides, although partial hydrolysis may release peptides very similar to the targets for both proteases. In cluster 3, α12 is fully embedded in α10. Nevertheless, both peptides have centrally located target AAs of all three proteases, making them unlikely products of hydrolysis. However, placement of AAs in the terminal regions may make them decent targets for partial hydrolysis by all three proteases. Cluster 4 contains a single peptide (γ36) and is found in the region of patatin immediately following cluster 1. Hydrolysis with Tryp would introduce a four AA N-terminal elongation and a potential one AA truncation in the C-terminal, although the Pro may also reduce efficiency (Giansanti et al., 2016). Although target AAs for both Alc and Neut are found through the peptide, the positioning of Phe residues at the termini makes γ36 a good target for partial hydrolysis. This may particularly be the case for Alc, as there are substantially fewer target AAs for this protease in the sequence compared to Neut. In clusters 5–7, target peptides have unfavourable positioning of target AAs for all three proteases, but partial hydrolysis by Alc and Neut may be possible for obtaining peptides closely resembling the target.

Ultimately, the *in silico* analysis shows that particularly cluster 1 is an excellent target for hydrolysis with Tryp. Tryp may also produce a peptide closely resembling γ36 from cluster 4. For the remaining clusters, no clear evidence for release of target (or closely related peptides) was found, although both Alc and Neut may produce hydrolysates containing peptides resembling the targets through partial hydrolysis, where Alc may produce peptides with better emulsifying properties than Neut.

3.2. Enzymatic hydrolysis

To validate the approach and benchmark the method of targeted hydrolysis, all available proteases were applied experimentally. Initially, enzymatic hydrolysis was performed without heat denaturation due to the high (90%) protein solubility (Table 2) in the native PPI (method A). However, a very low efficiency of hydrolysis was observed. The low degree of hydrolysis was observed in the lyophilized supernatant following post-hydrolysis heat inactivation of the proteases and subsequent centrifugation (Fig. 3A), by comparison to the control (unhydrolyzed PPI). Only for high concentrations of Flav (Fig. 3A, lane 12) and to a lesser extent Alc (Fig. 3A, lane 9), some degree of hydrolysis of the patatin band (~40 kDa) could be observed. This can be ascribed to the maintained inhibitory activity of wide variety and high abundance of protease inhibitors inherent to potato tubers (Kunitz-type ~20 kDa, PIN-type ~15 kDa, and MCPI-type ~5–10 kDa). It has been suggested that in a temperature range of 55–70 °C, inhibitor activity of protease inhibitors in potato protein is remarkably destroyed (Van Koningsveld et al., 2001). However, it has also been shown that even after cooking of potato protein at high temperature (75–100 °C), around 10% of the chymotrypsin inhibiting activity remains (Huang, Swanson, & Ryan, 1981). Application of harsh treatments, such as combination of thermal coagulation and acid precipitation, may therefore destroy inhibitory activity of some protease inhibitors (including aspartate-, cysteine-, and Kunitz-type protease inhibitors), while other protease inhibitors may retain their inhibitory function (Waglay & Karboune, 2016a). This is particularly of interest, as PTN 6.0S has been reported to exhibit chymotrypsin activity (Nongonierma, Paolella, Mudgil, Maqsood, & FitzGerald, 2017). Wang and Xiong (2005) investigated hydrolysis of heat-denatured potato protein by SDS-PAGE, and after 30 min Alc

Table 2
Bulk, physical properties of potato protein hydrolysates. For each PPH, the degree of hydrolysis (DH) by α-amino-N determination and the associated average peptide chain length (PCL) are indicated along with protein content (% by N*6.25), hydrolysis yield (%mass in freeze-dried supernatant), bulk density, whiteness, and solubility (at 10 mg/mL). For comparison, bulk properties for the initial substrate (potato protein isolate, PPI), sodium caseinate (SC), and a purified patatin fraction are listed.

Enzyme	E/S ratio (%)	DH (%)	PCL	Protein content (%)	Yield (%)	Bulk Density (g/mL)	Whiteness	Solubility (%)	Final pH
Neutrase	0.1	2.7 ± 0.1^{d}	36.6 ± 1.4^{b}	80.1 ± 0.6^{b}	15.1	0.27	68.0 ± 0.5^{d}	91.1 ± 1.1^{f}	7.40
	1.0	5.4 ± 0.5^{bc}	18.1 ± 0.9^{c}	84.3 ± 0.3^{a}	26.1	0.27	70.7 ± 0.5^{c}	99.2 ± 0.6^{ab}	7.25
	3.0	10.8 ± 1.2^{a}	9.2 ± 0.2^{d}	83.9 ± 1.3^{a}	39.9	0.21	68.2 ± 0.3^{d}	99.6 ± 0.1^{a}	6.80
Alcalase	0.1	1.2 ± 0.0^{e}	86.8 ± 7.2^{a}	71.6 ± 0.3^{d}	9.7	0.11	70.2 ± 0.8^{c}	98.7 ± 2.5^{ab}	7.68
	1.0	5.1 ± 0.4^{c}	19.2 ± 1.2^{c}	74.0 ± 0.3^{c}	13.9	0.13	71.5 ± 0.4^{c}	98.7 ± 0.1^{ab}	7.45
	3.0	6.2 ± 0.5^{b}	15.8 ± 1.1^{cd}	73.8 ± 0.3^{c}	17.5	0.18	71.3 ± 0.6^{c}	97.3 ± 1.8^{bc}	7.20
Flavourzyme	0.1	1.3 ± 0.1^{e}	71.9 ± 17.3^{a}	69.2 ± 0.4^{e}	8.8	0.24	66.2 ± 0.9^{d}	93.8 ± 2.3^{e}	8.0
	1.0	2.7 ± 0.9^{d}	36.9 ± 3.8^{b}	69.7 ± 0.0^{e}	12.4	0.24	63.0 ± 1.3^{e}	95.1 ± 1.5^{de}	7.86
	3.0	2.9 ± 0.6^{d}	35.4 ± 5.1^{b}	67.4 ± 0.1^{f}	14.4	0.43	59.3 ± 0.5^{f}	96.6 ± 3.5^{cd}	7.83
Trypsin	0.1	1.4 ± 0.1^{e}	70.7 ± 5.1^{a}	68.7 ± 0.2^{e}	9.1	0.13	66.6 ± 0.4^{d}	100.0 ± 0.0^{a}	7.85
	1.0	2.9 ± 0.2^{d}	34.9 ± 1.6^{b}	79.7 ± 2.1^{b}	19.5	0.10	68.4 ± 0.3^{d}	100.0 ± 0.0^{a}	7.53
	3.0	5.4 ± 0.7^{bc}	18.1 ± 1.2^{c}	83.4 ± 0.7^{a}	29.2	0.13	70.1 ± 0.6^{c}	96.5 ± 0.2^{cd}	7.24
PPI[a]		N/A	N/A	87.0 ± 0.2	N/A	0.29	79.8 ± 0.2^{b}	90.4 ± 0.7^{f}	N/A
SC[b]		N/A	N/A	92.6[c]	N/A	0.48	86.5 ± 0.0^{a}	99.6 ± 0.2^{ab}	N/A
Patatin		N/A	N/A	~95[d]	N/A	0.25	79.4 ± 0.3^{b}	98.9 ± 0.1^{ab}	N/A

Mean ± SD. data are based on three replicates where possible.
Different small superscript letters in each column indicate the significant differences among means at 95 confidence level (α = 0.05).
[a] Potato protein isolate (native, before heat treatment).
[b] Sodium caseinate (Miprodan 30, Arla, Denamrk).
[c] (Bjornshave et al., 2019).
[d] Lihme Protein Solutions provided information (based elemental analysis and a N-to-protein conversion factor of 6.25) following patatin purification.

hydrolysis, the ~40 kDa band vanished as a result of patatin hydrolysis (Wang & Xiong, 2005). Based on this, we hypothesized that the efficiency of enzymatic hydrolysis will be enhanced if the protease inhibitors become thermally denatured and hence, method B was employed. Although increased hydrolysis is desired, the degree of hydrolysis (DH) should be kept low, preferably lower than 10%, as peptides should be above a certain length to retain emulsifying properties. (Klompong, Benjakul, Kantachote, & Shahidi, 2007; Q. Liu, Kong, Xiong, & Xia, 2010; Morales-Medina, Tamm, Guadix, Guadix, & Drusch, 2016; Tamm et al., 2015). Consequently, the hydrolysis time was kept short (2 h) for method B.

Enzymatic hydrolysis was conducted in a free fall pH mode, i.e., the initial pH was adjusted at 8.0, but during hydrolysis gradually decreased at varying extent to a final pH of 6.8–8.0 for method B (Table 2). This was done to emulate industrial scale-up, where pH control may not always be possible (Kamnerdpetch et al., 2007). As expected, a relation between the extent of hydrolysis (DH) and the decrease in pH was observed. All hydrolysates displayed DH within the desired range (DH<8%) with the exception of 3% Neut showing significantly ($p < 0.05$) higher extent of hydrolysis (DH = 11%). Lower DH for Flav has also been observed in other studies investigating proteolysis of plant proteins (Li et al., 2015; Zhao et al., 2012). As expected, increasing E/S ratio increased the efficiency of enzymatic reaction significantly ($p < 0.05$), but at different extents. This is supported by SDS-PAGE analysis (Fig. 3B), where a substantial decrease of unhydrolyzed protein, compared to the non-denatured PPI (Fig. 3A), can be observed particularly for higher E/S ratios. This is in agreement with previous studies, where using fixed, initial substrate concentration and hydrolysis time, an increased E/S ratio also increases DH (Waglay & Karboune, 2016a).

Higher proteolytic activity for Flav, compared to e.g. Alc (DH of 22% vs. 8%), has previously been reported for hydrolysis of potato pulp but substantial differences in hydrolysis conditions (E/S ratio and time) complicate direct comparison. (Kamnerdpetch et al., 2007). Wang and Xiong (2005) investigated the hydrolysis of heat-denatured potato protein using Alc (1% E/S ratio) and obtained a DH of 0.72–2.3% over 0.5–6h, comparable to the DH obtained using Alc in our study. Although Alc is often reported to result in higher DH due to broader specificity (Demirhan, Apar, & Özbek, 2011; García Arteaga, Apéstegui Guardia, Muranyi, Eisner, & Schweiggert-Weisz, 2020; O'Keeffe & FitzGerald, 2014), a significantly higher ($p < 0.05$) DH is observed for Neut. This despite the initial pH of the hydrolysis is better aligned with optimum conditions for Alc. The lower DH for Alc is, however, in line with previous studies on potato protein hydrolysis (Kamnerdpetch et al., 2007; Wang & Xiong, 2005). Because a substantial amount of protease inhibitory activity is retained even after heating (Van Koningsveld et al., 2001), the mode of action for the applied proteases (i.e. protease families/classes) and the composition of protease inhibitors in PPI becomes a limiting step. Alc is a serine protease in the subtilisin family (Aldred, Phang, Conlan, Clare, & Vancso, 2008; Donlon, 2007) while Neut is a Zn-metalloprotease (J. Wu & Chen, 2011) but both exhibit endoproteolytic activity. As previously reported (García-Moreno, Gregersen, et al., 2020), protease inhibitors constitute more than half of the protein in the PPI (referred to as KMC-Food) used as substrate for hydrolysis. The vast majority of these are Kunitz-type inhibitors, where the class of serine protease inhibitors (KTI-B) constitute a very large proportion, corresponding to around 20% of the total protein (Pęksa & Miedzianka, 2021). In contrast, metalloprotease inhibitors constitute a very small part (>0.1%) and, importantly, are all in the form of metallocarboxypeptidase inhibitors (MCPI), thereby inhibiting exoproteolytic activity (Jørgensen et al., 2011; Pouvreau et al., 2001). Consequently, retained inhibitory activity against e.g. serine protease like Alc may likely explain why a significantly higher DH is observed for Neut. Interestingly, DH also appears to be somewhat correlated with both protein content in the PPH and the yield of hydrolysis (Table 2), indicating that hydrolysis is indeed a prerequisite to resolubilise the heat-denatured PPI, in line with previous studies (Miedzianka et al., 2014; Wang & Xiong, 2005). The significantly lower DH ($p < 0.05$) observed for Flav is also reflected in significantly lower ($p < 0.05$) protein content and lower yields at all E/S ratios. Low yields (<20%) and a substantial reduction in protein content (<80%) compared to PPI (87%) is also observed for Alc and Tryp at low E/S ratios (0.1 and 1%), thereby making such processes potentially unbeneficial from an industrial and economical point of view.

3.3. Bulk properties of PPH

Overall, hydrolysis decreased the bulk density and whiteness compared to the PPI, but improved solubility (Table 2). A more elaborate discussion on basic physical characterization of PPHs may be found in the supplementary information.

3.3.1. Emulsifying properties

In general, application of lower E/S ratios (0.1% and 1%) resulted in significantly lower EAI (Table 3) compared to controls (PPI, SC and Pat) ($P < 0.05$), and only Tryp 1% displayed EAI comparable to PPI and SC ($P > 0.05$) but still significantly lower than native Pat ($P < 0.05$). In contrast, the EAI of Tryp PPHs at 3% E/S ratio was significantly higher ($P < 0.05$) compared to both PPI and SC and comparable to the EAI of native Pat ($P > 0.05$), confirming the original hypothesis based on *in silico* analysis. 3% Alc PPH also displayed EAI higher than PPI and SC ($P < 0.05$) but was significantly lower than both Pat and 3% Tryp PPH ($P < 0.05$). At 3% E/S ratio, Flav treatment resulted in a nearly equivalent ($P > 0.05$) EAI compared to those from PPI and SC, while Neut PPH displayed the lowest EAIs ($P < 0.05$). That isolated, native Pat has strong emulsifying properties is in line with previous studies (Van Koningsveld et al., 2006). Using other methods to evaluate emulsifying properties than EAI (e.g. emulsion droplet size distribution and oil/water interfacial tension reduction) has, however, revealed that native Pat may not result in such strong emulsification as observed here, whereas the 3% Tryp PPH does appear to indeed have very strong emulsifying properties regardless of evaluation method (Data not shown, manuscript submitted). In any case, obtaining native, isolated patatin is a costly process, and therefore not a scalable and economically viable solution.

All PPHs in our study produced emulsions with higher ESI compared to those with PPI, SC and Pat ($P < 0.05$). The highest ESI value was determined for Neut (67.0 min) followed by Flav (44.5 min), both at 1% E/S. However, these PPHs also displayed the lowest values of EAI across all PPHs. EAI does not follow the same trend as a function of E/S ratio (and thus DH) for the investigated proteases. For instance, in case of Neut and Flav by increasing the E/S ratio from 0.1% to 1%, the EAI values decreased, whereas it increased significantly at 3% E/S ($P < 0.05$). On the other hand, the EAI of Tryp derived PPH, showed a constantly increasing trend with increasing enzyme concentration, reaching 124 m^2/g at 3% E/S (corresponding to DH = 5.4%). EAI values of Alc derived PPH showed no significant difference between 0.1 and 1% E/S ratio ($P > 0.05$), whereas it increased significantly ($P < 0.05$) to 109 m^2/g at 3% E/S (DH = 6.2%). Similarly, previous studies have shown that soy protein hydrolysates produced with Tryp (DH 1–2%) exhibited a better EAI than those of hydrolyzed by Neut at the same DH (X. Zhao & Hou, 2009). This could be ascribed to the higher specificity of Tryp, resulting in a more well-defined hydrolysate and release of peptides containing a hydrophilic C-terminus (Lys/Arg), which could contribute to electrostatic stabilization of the oil droplets in the emulsion (X. Zhao & Hou, 2009). A recent study on casein hydrolysates similarly found that, compared with Alc and Neut, low DH (~5%) hydrolysates produced with Tryp showed superior emulsifying properties, which was ascribed to a higher proportion of amphiphilic peptides (Yu, Zheng, Cai, Zhao, & Zhao, 2022). In addition, other studies have identified superior solubility and emulsifying properties of protein hydrolysates produced with Tryp (Padial-Domínguez, Espejo-Carpio, Pérez-Gálvez, Guadix, & Guadix, 2020; Taherian, Britten, Sabik, & Fustier, 2011).

Overall, EAI and ESI did not correlate with DH nor each other directly (Fig. A.3). Diffusion properties in solution highly influence the adsorption rate of emulsifiers to the oil-water interfaces during homogenization (McClements & Jafari, 2018). In other words, there is a propensity for smaller monomers to diffuse more quickly to an interface than larger proteins or aggregates. Despite a significantly higher DH for Neut at 3%, the EAI was less than half of the EAI for Alc- and Tryp-derived PPHs (corresponding to DH = 6.2% and DH = 5.4%, respectively). In contrast, Flav-derived PPHs displayed much lower DH (2.9%) but higher EAI than Neut PPHs. This indicates that although smaller peptides diffuse rapidly and adsorb at the interface, they may indeed be less efficient in stabilizing emulsions and thus, mean peptide chain length (PCL) cannot be used directly as an indicator of emulsification potential, as previously shown in potato protein hydrolysates (Akbari, Mohammadzadeh Milani, & Biparva, 2020). Previous studies have indicated that a minimum length (>12 AAs) is required for a peptide to obtain a defined structure at the interface and thus display emulsifying properties (García-Moreno, Gregersen, et al., 2020), indicating that there may be a preferred length range for peptides to display emulsifying properties. Although there are no clear trends in our data, it does appear that operating within a range of fairly low DH (~2–8%) seems to promote the likelihood of obtaining a hydrolysate with improved emulsification, when evaluated by EAI and ESI (Fig. A.3.A and Fig. A.3.B), but this also appears to be highly protease-dependent and not universally applicable. Interestingly, there are also indications, but no strong evidence, that there may be a trade-off between EAI and ESI for the hydrolysates (Fig. A.3.C). Although DH (and thus PCL) is not a viable measures to estimate emulsifying activity by itself, it may be one of many factors to consider; particularly in relation to avoiding excessive hydrolysis, which can substantially deteriorate emulsifying activity (Klompong et al., 2007; Q. Liu et al., 2010; Vioque, Sánchez-vioque, Clemente, Pedroche, & Millán, 2000). The amphiphilicity and interfacial conformation of peptides may, ultimately, outweigh peptide length as a determining factor for emulsifying properties (Klompong et al., 2007).

Importantly, our results indicate that Tryp is indeed capable of producing a PPH with significantly improved emulsifying properties compared to both other industrially relevant proteases and the substrate itself. In fact, only the application of Tryp was able to improve both emulsification activity and stability significantly ($P < 0.05$), compared to untreated PPI, validating our hypothesis. This highlights that a data-driven, targeted approach for enzymatic hydrolysis is a promising approach for improving the functional parameters of industrial side

Table 3
Emulsifying and foaming properties of potato protein hydrolysates (PPH). For each PPH, the Emulsification Activity Index (EAI), Emulsification Stability Index (ESI), Foaming Capacity (FC), and Foaming Stability (FS) are indicated. For comparison, the native potato protein isolate (PPI), sodium caseinate (SC), and a purified patatin fraction are listed.

Enzyme	E/S ratio (%)	EAI (m^2/g)	ESI (min)	FC (%)	FS (%)
Neutrase	0.1	45.1 ± 0.4^{f}	22.7 ± 2.1^{fg}	100±8^{g}	28.0 ± 3.4d^{c}
	1.0	33.3 ± 2.9^{g}	67.1 ± 3.3^{a}	138 ± 10^{e}	20.4 ± 4.4d^{de}
	3.0	52.4 ± 4.6^{ed}	25.5 ± 2.6^{ef}	98±6^{g}	21.6 ± 1.5^{fd}
Alcalase	0.1	54.7 ± 4.3^{d}	21.9 ± 0.4^{fg}	288 ± 10^{d}	6.9 ± 1.2^{gh}
	1.0	52.2 ± 0.5^{ed}	26.8 ± 2.1^{e}	498 ± 10^{a}	5.4 ± 0.5^{h}
	3.0	109.5 ± 1.4^{b}	20.1 ± 1.7^{gh}	501±2^{a}	7.4 ± 0.5^{gh}
Flavourzyme	0.1	48.4 ± 2.6^{ef}	31.8 ± 3.7^{cd}	380±8^{c}	8.4 ± 0.9^{gh}
	1.0	30.8 ± 3.5^{g}	44.6 ± 1.6^{b}	301 ± 10^{d}	7.5 ± 0.6^{gh}
	3.0	68.0 ± 2.8^{c}	35.7 ± 2.3^{c}	400±4^{b}	5.7 ± 1.2^{gh}
Trypsin	0.1	42.4 ± 4.0^{f}	31.0 ± 0.5^{d}	300±8^{d}	9.3 ± 1.5^{gh}
	1.0	66.5 ± 1.9^{c}	20.8 ± 1.2^{gh}	401±6^{b}	12.3 ± 0.6^{fg}
	3.0	124.2 ± 4.9^{a}	25.2 ± 2.3^{ef}	498±2^{a}	15.8 ± 0.5^{ef}
PPI**		70.3 ± 4.1^{c}	18.1 ± 1.9^{hi}	120±6^{f}	65 ± 0.5^{a}
SC***		64.5 ± 3.3^{c}	15.9 ± 1.2^{i}	90±2^{g}	47.1 ± 3.3^{b}
Patatin		127.2 ± 1.5^{a}	11.8 ± 1.1^{j}	53±2^{h}	65.2 ± 6.9^{a}

Mean ± SD. all data are based on three replicates.
Different small superscript letters in each column indicate the significant differences among means at 95 confidence level ($\alpha = 0.05$).
* Freeze-Dried potato protein hydrolysate (supernatant after centrifugation).
** Potato protein isolate (native, before heat treatment).
*** Sodium caseinate.

streams such as potato protein. And that this may be obtained in a predictable manner, alleviating the need for conventional trial-and-error methodology.

3.3.2. Foaming properties

With the exception of Neut-derived PPHs at 0.1% and 3% E/S, all PPHs showed significantly higher ($P < 0.05$) FC compared to control samples. In contrast to the emulsifying properties, the highest FC of the control samples was determined for PPI, followed by SC, and patatin, respectively ($P < 0.05$). The PPHs from Alc and Tryp showed remarkably high (~500%) but comparable ($P > 0.05$) FC at high E/S ratio (3%) (Table 3), but no direct correlation between foaming capacity and DH (Fig. A.4.A). Conformational properties of released peptides relies highly on the specificity of the applied protease. For instance, the lower FC as well as EAI of Neut-derived PPH may be attributed to a sequence-specific and lower surface activity of released peptides rather than their average length; similarly as was observed for emulsifying properties. That being said, the decrease in FC with a decrease in E/S ratio from 1% to 3% may also be the result of extensive hydrolysis, ultimately releasing too short peptides with a decreased propensity to form defined structures at the interface. This is in agreement with previous studies on Alc hydrolysis of a potato protein isolate, where extending hydrolysis time, increased DH up to 17%, which resulted in a decrease in FC (Akbari et al., 2020). Such high DH was not observed for Alc (or other) PPHs in this study, which could explain why the effect was only seen for Neut-derived PPHs as all other PPH had a DH in the range from 1.2% to 6.2% (Table 2).

Control samples showed higher ($P < 0.05$) stability compared to PPHs (Table 3), as the highest FS (~65%) was determined for the native PPI and the patatin fraction ($P > 0.05$), followed by SC at ~47% ($P < 0.05$). For PPHs, the highest FS was determined for Neut followed by Tryp PPHs, while both Alc and Flav PPHs presented the lowest FS (<10%) among all ($P < 0.05$). Increasing the Neut E/S ratio from 0.1% to 3% caused a significant decrease ($P < 0.05$) in stability of formed foams from 28% to about 22% ($P < 0.05$), whereas the inverse effect was observed for Tryp, where increasing E/S from 0.1% to 3% significantly increased FS from ~9% to ~16% ($P < 0.05$). Between Alc and Flav PPHs, there was no significant difference ($P > 0.05$) in determined FS. Interestingly, only hydrolysis by Tryp improved both FC and FS (as well as EAI) with increasing DH. In earlier studies, the FC and FS of a potato protein concentrate (8% and 5.3%, respectively) increased to 162% and 51% after hydrolysis by Alc for 2h (Miedzianka et al., 2014). Although these values are not in full agreement with our data, the study also highlights the positive effect of proteolysis for increasing the surface activity, as well as solubility, compared to the protein substrate. In our study, Alc and Tryp hydrolysis at 3% E/S ratio resulted in both comparable FC (~500%) and DH (~6%), but remarkably different FS. Foams produced with 3% Tryp PPH had double the stability of 3% Alc-derived PPH (Table 3). No apparent relation between DH and FS was observed (Fig. A.4.B).

Similarly to the relation between EAI and ESI, there appears to be a general trade-off between FC and FS (Fig. A.4.C), although e.g. Tryp PPHs shows the opposite trend. While control samples (PPI, SC, and Pat) produce the most stable foams, they produce the least stable emulsions. Hydrolysis of PPI (as well as native Pat) significantly increases the capacity to foam ($P < 0.05$), but also significantly decreases the foam stability ($P < 0.05$), in line with the general observations of a negative relation between FC and FS for PPHs in this study. Although no clear correlation is observed, there does appear to be some relation between high emulsifying and foaming capacities (Fig. A.5.A), indicating that to some extent, similar molecular properties are involved in both interfacial properties, in line with previous studies (Wouters, Rombouts, Fierens, Brijs, & Delcour, 2016). The stability of the interfaces, however, appear to be governed by different forces and properties as no apparent relation is observed (Fig. A.5.B).

Overall, the PPHs (particularly 3% Tryp) show strong emulsifying and foaming properties. Other studies using the same assays to evaluate these properties of hydrolysates generally found comparable and often lower values for diverse protein sources such as sea cucumber collagen (Z. Liu, Su, & Zeng, 2011), lentil protein isolate (Avramenko, Low, & Nickerson, 2013), pea protein isolate (Barac et al., 2012), whey and soy protein (Padial-Domínguez et al., 2020), soy (Chen et al., 2019; Liang et al., 2020), chickpea (Mokni Ghribi et al., 2015), sweet potato (Falade, Mu, & Zhang, 2021). Although some studies do present superior metrics on interfacial properties, it should be noted that substantially higher hydrolysate concentrations (>0.5% w/v) were used, which makes direct comparison difficult. Some studies also show a significant pH-dependency for interfacial properties (Ruiz-Álvarez et al., 2022), and this aspect should be investigated further for PPHs to establish optimal conditions and applications for their use.

3.4. Peptide identification and mean peptide properties

Across the 12 PPHs investigated with LC-MS/MS, unspecific analysis in MaxQuant resulted in identification of 46,316 unique peptides following removal of reverse and contaminant peptides. Although a higher FDR (5%) was applied for MaxQuant analysis, this level was previously shown to be suitable for non-specific digests due to the significantly increased combinatorial search space (Gregersen et al., 2022). In general, a lower number of peptides were identified in PPHs produced using Neut, although more than 10,000 peptides were identified in all PPHs (Table 4). This is a tremendous increase in depth of analysis compared to previous reports of LC-MS/MS analysis on hydrolysates, where the number of identified peptides is often reported in the tens to low thousands range (Caron et al., 2016; Cui, Sun, Cheng, & Guo, 2022; Hinnenkamp & Ismail, 2021; Y. P. Huang, Dias, Leite Nobrega de Moura Bell, & Barile, 2022; Jafarpour, Gregersen, et al., 2020; Jin, Yan, Yu, & Qi, 2015; M. Li, Zheng, Lin, Zhu, & Zhang, 2020).

As expected, changing hydrolysis conditions by increasing E/S ratio, and thereby increasing DH, had a substantial effect on the number and nature of identified peptides for all four investigated proteases. This is illustrated both by the number of identified peptides (Table 4) as well as shared peptides between PPHs obtained using the same protease (Fig. A.6). Interestingly, the effect of protease and E/S ratio on DH, determined through α-amino nitrogen quantification (Table 2), is not to the same extent reflected in the peptide level data, using intensity-weighted peptide abundance estimation, PCL_{avg} (Table 4). This is in contrast to previous studies, where a much stronger correlation between

Table 4
Summary statistics for LC-MS/MS peptidomic analysis. For each PPH, the number of identified peptides (Peptide IDs) and intensity-weighted average peptide length (PCL_{avg}) from unspecific analysis of LC-MS/MS data in MaxQuant are indicated. The total peptide MS1 intensity (Σ Int) for each PPH is listed along with the associated normalization factor (NF) used for relative, peptide-level comparison.

Enzyme		Alcalase		Flavourzyme			Neutrase			Trypsin		
E/S ratio	0.1%	1%	3%	0.1%	1%	3%	0.1%	1%	3%	0.1%	1%	3%
Peptide IDs	13140	14106	13125	14622	12936	13094	12210	11944	10829	14948	12756	12475
Total		19513			21976			17356			23509	
PCL_{avg}	15.9	15.3	14.9	15.8	14.8	14.5	14.2	13.2	12.7	15.9	15.8	15.0
Σ Int [$1E^{12}$]	8.7	12.2	13.2	6.9	5.5	8.1	13.6	12.0	9.3	5.7	10.6	13.7
NF	0.638	0.889	0.966	0.502	0.399	0.589	0.996	0.877	0.683	0.420	0.773	1

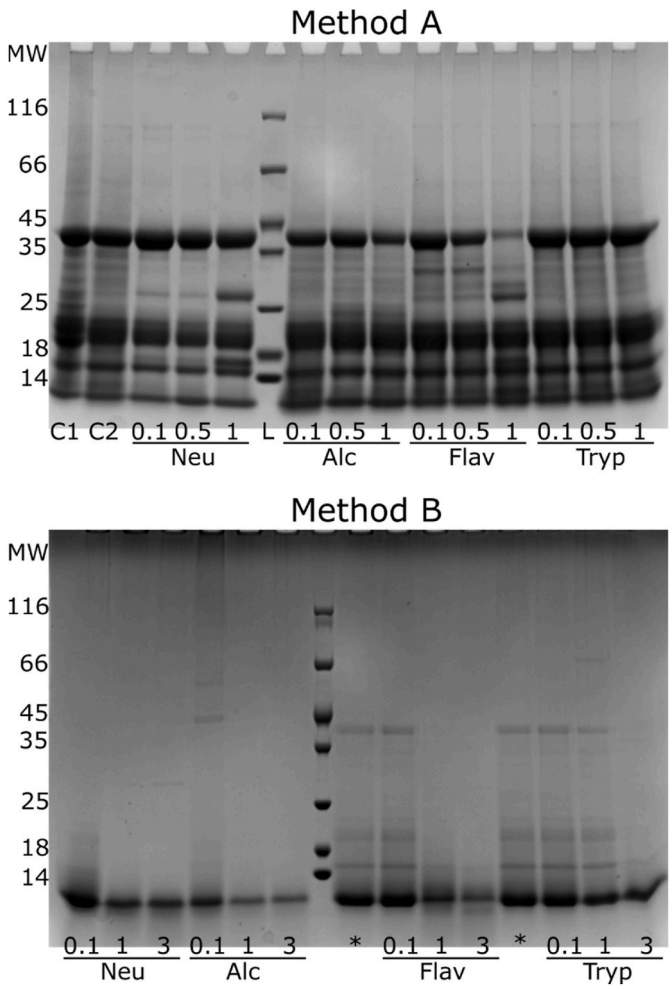

Fig. 3. SDS-PAGE analysis of PPH (freeze-dried supernatants) following hydrolysis of native PPI (Method A) and heat denatured PPI (Method B) using Neutrase (Neu), Alcalase (Alc), Flavourzyme (Flav), or Trypsin (Tryp) at different E/S ratios (Method A: 0.1%, 0.5%, and 1%. Method B: 0.1%, 1%, and 3%). C1: Native PPI. C2: Process control with native PPI. *Repetition of 0.1% hydrolysis for Flav and Tryp.

the two methods was observed (Jafarpour, Gregersen, et al., 2020). However, there are notable differences between the two studies. In Jafarpour, Gomes, et al. (2020), hydrolysis was performed on a raw side stream from the cod industry, where this study deals with a much purer protein isolate. This is clearly illustrated by the lack of distinct protein bands in SDS-PAGE analysis in the cod hydrolysates, where we here observed strong bands from intact protein and larger protein fragments by SDS-PAGE following hydrolysis (Fig. 3), indicating that a substantial amount of protein remains in forms undetectable using a bottom-up proteomics approach. According to Linderstrøm-Lang theory, proteases may have higher affinity for intermediate fragments/peptides than intact proteins (Adler-Nissen, 1986; Linderstrøm-Lang, 1953). It was previously shown in e.g. milk (Deng, van der Veer, Sforza, Gruppen, & Wierenga, 2018; Hinnenkamp & Ismail, 2021) and rice (Nisov, Ercili-Cura, & Nordlund, 2020) as well as potato (Akbari et al., 2020; Pęksa & Miedzianka, 2014) proteins, that this is indeed the case in a highly protein- and protease-specific manner. This also suggests that the observation of intense bands for residual intact protein by SDS-PAGE (Fig. 3), should likely not be interpreted as lack of hydrolytic activity, but rather increased protease affinity for intermediate fragments/peptides. Similarly, hydrolysis to the single AA and dipeptide level will contribute significantly to the total DH of a sample, while these remain undetected in the MS experimental design. Nevertheless, a decrease in PCL_{avg} is observed with increasing E/S ratio for each protease, and substantially lower PCL_{avg} values are obtained for Neut corresponding to the higher DH in these PPHs. This shows that even in spite of the challenges imposed by intact protein and other undetected species, MS data and PCL_{avg} can provide an indication for the progression of hydrolysis in addition to peptide- and protein-level insight.

3.5. Identification of known peptide emulsifiers from potato proteins

Based on emulsifying properties of the PPHs, a deeper peptide-level analysis of peptides associated with the seven sequence clusters associated with known and highly potent emulsifiers (Section 3.1) was performed. As the major constituents of the potato proteome (i.e. patatin and protease inhibitors) all represent a large number of protein isoforms, mapping peptides to the isoforms is a challenging task. This is particularly the case as single AA substitutions and minor truncations/elongations may not have a detrimental effect on the peptide functionality (Enser et al., 1990; García-Moreno, Gregersen, et al., 2020; García-Moreno, Jacobsen, et al., 2020; Ricardo et al., 2021). To accommodate this, we established a workflow, where identified peptides were mapped onto representative target cluster sequences (Fig. 2) by defining lead protein sequence clusters (Table 1). The workflow allows for determining the degree of overlap between identified peptides and the representative cluster sequence while allowing for substitutions, truncations, and elongations. By using the peptide MS1 intensity as an estimate of abundance, it is thus possible to determine how much of the peptide MS1 intensity for the whole PPH is constituted by peptides adhering to both the length requirement and a minimum sequence overlap with a given target cluster. As the total MS1 intensity varies substantially between PPHs (Table 4), unhydrolyzed proteins content varied between PPHs (Fig. 3), and as the same total amount was loaded on-column (1 μg), total MS1 intensities were normalized relative to the PPH with the highest MS1 intensity (Tryp 3%). After applying the normalization factors (Table 4), the normalized, relative MS1 intensity constituted by peptides with >50%, >75%, and >95% overlap with each of the seven target clusters, was determined for each PPH using both a 12 AA (Fig. 4, left) and 15 AA (Fig. 4, right) minimum length requirement. From here, we see that peptides mapping to target peptide clusters 1 and 3 account for the largest contributions of mapped peptides regardless of required sequence overlap and length requirement. We also see that peptides mapping to clusters 2, 5, and 6 have practically no contribution to the sum, while the contribution from cluster 4 and 7 peptides is low. Moreover, we observe a shift in which PPHs has the highest relative contribution to overlapping peptides, based on the requirement of degree of overlap.

Interestingly, target cluster overlap (Fig. 4) overall shows low agreement with observed emulsifying properties of the PPHs (Table 3). While a low degree of overlap (>50%) shows that Alc PPHs (particularly at 1% and 3% E/S which also show high EAI) has the highest proportion of overlapping peptides, increasing requirement of sequence overlap shift the highest proportion of overlapping peptides towards Flav and Neut PPHs (which show lowest EAI), while Alc PPHs here show the lowest proportion. In all cases, Tryp PPHs (showing highest EAI), show an intermediate proportion of overlapping peptides in comparison and a low content of cluster 1 peptides, which were the primary target by Tryp hydrolysis. This observation led us to investigate if certain regions of a target cluster may be more important. By extracting the sequences for high intensity peptides in each PPH with >50% overlap in cluster 1 and 3 (Table A.3), it is possible to see that Neut PPHs contain abundant peptides overlapping with cluster 1, but that all are located in the C-terminal region of the cluster (Fig. 5, left). In contrast, high intensity Alc peptides are found in the N-terminal region of the cluster. While high intensity Flav peptides are located in both cluster termini, Tryp PPH peptides, particularly at 3% E/S, span more of the cluster (Fig. 5, left). This indicates that the N-terminal region of the cluster may be of higher importance, and, more importantly, that peptides also should cover at

12AA minimum length

		Alcalase			Flavourzyme			Neutrase			Trypsin		
		0.1%	1%	3%	0.1%	1%	3%	0.1%	1%	3%	0.1%	1%	3%
>50%	C1	2.6%	5.9%	6.7%	2.1%	4.9%	7.0%	1.4%	2.3%	1.4%	1.8%	0.7%	0.9%
	C2	0.0%	0.0%	0.0%	0.0%	0.0%	0.0%	0.0%	0.2%	0.3%	0.0%	0.1%	0.1%
	C3	6.8%	11.3%	8.9%	4.1%	3.5%	4.3%	5.0%	4.5%	3.5%	3.9%	4.9%	3.8%
	C4	2.0%	2.8%	3.1%	1.9%	1.8%	2.4%	2.5%	2.0%	1.0%	1.4%	1.9%	3.2%
	C5	0.0%	0.0%	0.0%	0.0%	0.0%	0.0%	0.0%	0.1%	0.1%	0.0%	0.0%	0.0%
	C6	0.9%	0.8%	1.1%	2.5%	0.6%	1.0%	1.1%	0.1%	0.1%	1.9%	4.1%	3.0%
	C7	1.1%	2.3%	2.4%	0.7%	0.8%	1.2%	2.8%	1.6%	0.8%	0.6%	0.1%	0.2%
	Sum	13.4%	23.1%	22.4%	11.3%	11.7%	15.9%	12.8%	10.8%	7.1%	9.6%	11.9%	11.2%
>75%	C1	0.4%	0.7%	0.4%	0.9%	3.2%	5.8%	1.2%	2.1%	1.2%	0.7%	0.3%	0.7%
	C2	0.0%	0.0%	0.0%	0.0%	0.0%	0.0%	0.0%	0.1%	0.3%	0.0%	0.0%	0.0%
	C3	2.1%	3.1%	1.8%	3.6%	3.0%	3.7%	5.0%	4.4%	3.4%	3.5%	4.5%	3.6%
	C4	0.7%	0.8%	1.2%	0.9%	1.0%	1.2%	2.0%	1.7%	0.6%	0.8%	0.8%	1.2%
	C5	0.0%	0.0%	0.0%	0.0%	0.0%	0.0%	0.0%	0.0%	0.0%	0.0%	0.0%	0.0%
	C6	0.0%	0.0%	0.0%	0.0%	0.0%	0.0%	0.0%	0.0%	0.0%	0.0%	0.0%	0.0%
	C7	0.9%	1.8%	2.0%	0.6%	0.8%	1.1%	2.7%	1.5%	0.7%	0.6%	0.1%	0.1%
	Sum	4.0%	6.3%	5.4%	6.0%	8.0%	11.9%	11.0%	9.9%	6.3%	5.5%	5.8%	5.7%
>95%	C1	0.1%	0.2%	0.2%	0.2%	1.2%	1.5%	1.0%	1.5%	0.9%	0.2%	0.2%	0.7%
	C2	0.0%	0.0%	0.0%	0.0%	0.0%	0.0%	0.0%	0.0%	0.0%	0.0%	0.0%	0.0%
	C3	0.9%	0.6%	0.2%	2.9%	2.7%	3.2%	4.9%	4.4%	3.4%	3.0%	3.9%	3.5%
	C4	0.1%	0.2%	0.3%	0.3%	0.6%	0.5%	0.3%	0.7%	0.3%	0.3%	0.0%	0.0%
	C5	0.0%	0.0%	0.0%	0.0%	0.0%	0.0%	0.0%	0.0%	0.0%	0.0%	0.0%	0.0%
	C6	0.0%	0.0%	0.0%	0.0%	0.0%	0.0%	0.0%	0.0%	0.0%	0.0%	0.0%	0.0%
	C7	0.1%	0.2%	0.3%	0.4%	0.7%	0.9%	1.6%	1.1%	0.5%	0.3%	0.0%	0.0%
	Sum	1.1%	1.2%	1.0%	3.7%	5.1%	6.0%	7.8%	7.6%	5.1%	3.7%	4.2%	4.3%

15AA minimum length

		Alcalase			Flavourzyme			Neutrase			Trypsin		
		0.1%	1%	3%	0.1%	1%	3%	0.1%	1%	3%	0.1%	1%	3%
C1		2.3%	5.5%	6.2%	1.5%	2.8%	4.4%	1.3%	2.0%	1.1%	1.2%	0.6%	0.8%
C2		0.0%	0.0%	0.0%	0.0%	0.0%	0.0%	0.0%	0.1%	0.2%	0.0%	0.1%	0.1%
C3		5.6%	9.1%	7.2%	3.0%	1.5%	1.7%	4.6%	3.5%	2.4%	2.8%	3.5%	1.7%
C4		1.5%	2.4%	2.7%	1.0%	0.7%	1.0%	1.3%	1.2%	0.7%	0.8%	1.7%	2.9%
C5		0.0%	0.0%	0.0%	0.0%	0.0%	0.0%	0.0%	0.0%	0.0%	0.0%	0.0%	0.0%
C6		0.2%	0.1%	0.1%	0.8%	0.0%	0.1%	0.0%	0.0%	0.0%	0.6%	1.3%	0.7%
C7		1.0%	2.1%	2.3%	0.1%	0.1%	0.1%	1.1%	0.5%	0.2%	0.1%	0.1%	0.2%
Sum		10.7%	19.2%	18.5%	6.5%	5.2%	7.3%	8.3%	7.3%	4.5%	5.6%	7.2%	6.4%
C1		0.4%	0.5%	0.3%	0.7%	2.2%	3.9%	1.2%	1.8%	0.9%	0.5%	0.3%	0.7%
C2		0.0%	0.0%	0.0%	0.0%	0.0%	0.0%	0.0%	0.1%	0.2%	0.0%	0.0%	0.0%
C3		0.9%	0.9%	0.1%	2.5%	1.1%	1.2%	4.5%	3.4%	2.2%	2.5%	3.1%	1.6%
C4		0.3%	0.5%	0.8%	0.4%	0.3%	0.5%	0.9%	0.9%	0.3%	0.3%	0.6%	1.0%
C5		0.0%	0.0%	0.0%	0.0%	0.0%	0.0%	0.0%	0.0%	0.0%	0.0%	0.0%	0.0%
C6		0.0%	0.0%	0.0%	0.0%	0.0%	0.0%	0.0%	0.0%	0.0%	0.0%	0.0%	0.0%
C7		0.8%	1.6%	1.9%	0.1%	0.1%	0.1%	1.1%	0.4%	0.2%	0.1%	0.1%	0.1%
Sum		2.3%	3.5%	3.2%	3.7%	3.6%	5.7%	7.7%	6.6%	3.8%	3.4%	4.1%	3.4%
C1		0.0%	0.2%	0.1%	0.1%	0.4%	0.2%	1.0%	1.5%	0.9%	0.1%	0.2%	0.7%
C2		0.0%	0.0%	0.0%	0.0%	0.0%	0.0%	0.0%	0.0%	0.0%	0.0%	0.0%	0.0%
C3		0.3%	0.0%	0.0%	1.8%	0.7%	0.6%	4.4%	3.4%	2.2%	2.0%	2.4%	1.5%
C4		0.0%	0.1%	0.2%	0.1%	0.1%	0.0%	0.0%	0.0%	0.0%	0.0%	0.0%	0.0%
C5		0.0%	0.0%	0.0%	0.0%	0.0%	0.0%	0.0%	0.0%	0.0%	0.0%	0.0%	0.0%
C6		0.0%	0.0%	0.0%	0.0%	0.0%	0.0%	0.0%	0.0%	0.0%	0.0%	0.0%	0.0%
C7		0.0%	0.1%	0.2%	0.0%	0.0%	0.0%	0.1%	0.0%	0.0%	0.0%	0.0%	0.0%
Sum		0.4%	0.4%	0.5%	2.0%	1.2%	0.9%	5.5%	4.9%	3.1%	2.1%	2.7%	2.2%

Fig. 4. Heat maps (blue (low) to red (high)) of quantitative (by MS1 I_{rel}) sequence overlap between identified peptides and the target cluster sequences. For all seven target clusters (C1-C7), overlaps are given with increasing minimum overlap (50%, 75%, 95% (top to bottom)) and increasing minimum peptide length (12 AAs (left) and 15 AAs (right)) requirements. Sums across all clusters for each condition are color coded separately from the individual clusters to illustrate overall adherence of PPH peptides to all target clusters. (For interpretation of the references to color in this figure legend, the reader is referred to the Web version of this article.)

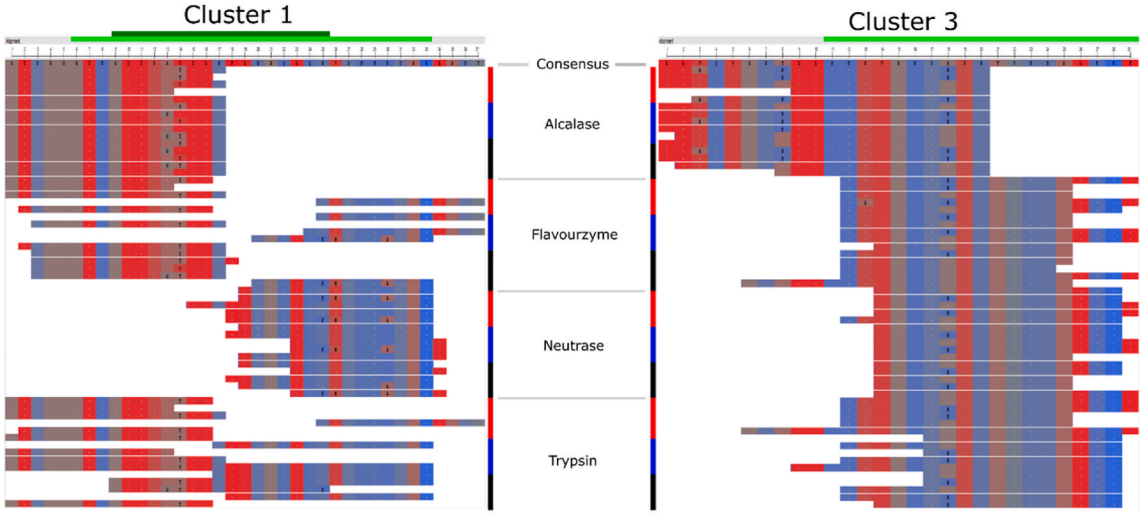

Fig. 5. Alignment of top-5 high intensity peptides in Alc, Flav, Neut, and Tryp (top to bottom) PPHs for 0.1% (red), 1% (blue), and 3% (black) E/S ratio. Only peptides with at least 50% overlap with the target cluster consensus sequence for Cluster 1 (left) and Cluster 3 (right) are shown. For each condition (protease and E/S ratio), the top-5 peptides are depicted with descending relative MS1 intensity (top to bottom). Amino acids are color coded from red (hydrophobic) to blue (hydrophilic) according to the NCBI MSA Viewer hydropathy color scale. The consensus sequence for each cluster is shown by a light green bar (top), while the suggested "core region" for cluster 1 peptides is shown in dark green. The consensus sequence was extended in both termini to allow for full mapping and visualization of all top-5 overlapping peptides. Single amino acid substitutions (relative to the consensus sequence) are assigned by the substituent single letter code on the individual peptide level. (For interpretation of the references to color in this figure legend, the reader is referred to the Web version of this article.)

least a certain part of the cluster to attain the interfacial activity. This is in agreement with previous studies (Yesiltas et al., 2021), where cluster 1 peptides (e.g. γ105) are highly truncated in the C-terminal region of the target cluster sequence. As such the region covered by γ105 (GIIPGTILEFLEGQLQK) may be regarded as the core region of cluster 1 and could represent a "critical region" for emulsifying activity, as this region produces a highly amphiphilic α-helix at the interface. With the exception of γ1 (which is cleaved by trypsin after Lys in position 3 resulting in γ75), all cluster 1 peptides (full length and/or full length isoforms) were identified in the 3% Tryp PPH (Table A.4). Some were also identified in the 1% Tryp PPH, while very minute amounts (<0.002% I_{rel}) were found in 3% Flav PPH, both verifying that target peptides were indeed released in a targeted manner and indicating that observed differences in emulsifying activity may potentially be ascribed to substantial presence of these highly functional peptides. Nevertheless, this type of analysis only describes a subpopulation of the entire, complex PPH, and does not account for all other peptides and their potential (positive or negative) contribution to the bulk functionality of the PPHs.

Our results also indicate that a quite substantial amount of Tryp was needed to efficiently release the peptides, which may be ascribed to residual inhibitory activity in the PPH despite heat treatment.

Cluster 3 peptides constitute the majority of all overlapping cluster peptides. With increasing requirements for both length and degree of overlap, the highest proportion shifts from Alc PPHs to Flav and particularly Neut and Tryp PPHs (Fig. 4). Cluster 3 represents two patatin-derived peptide emulsifiers, α10 and α12, which were previously shown to indeed adopt a helical conformation at the oil/water interface (García-Moreno et al., 2021). High intensity Flav, Neut, and Tryp peptides all appear to cover a significant amount of the target cluster sequence (Fig. 5, right), which intuitively should make all these PPHs good emulsifiers. Nevertheless, if assuming a helical conformation with 3.6 AA per turn, the distribution of AAs in these peptides do not appear favourable for producing an amphiphilic helix. Particularly high intensity Neut peptides are slightly truncated in the N-terminal region of the cluster, making the characteristic pattern of AA distribution in an amphiphilic helix (Eisenberg, Weiss, & Terwilliger, 1982) absent, to a large degree. In contrast, Alc peptides extend N-terminally of the consensus sequence in cluster 3. This means that peptides include a region, which have a highly favourable AA distribution for adopting a highly amphiphilic helical conformation at the interface, and also forms an amphipathic helix in native patatin (Fig. A.7). Furthermore, the most abundant cluster 3 peptides in Alc PPHs (Fig. 5, right) are variants of the same peptide (LLAQVGENLLKKPVSKDNPE), containing either single AA substitutions or minor (1–2 AA) N-terminal truncations, which are likely to not have substantial effect on the interfacial properties. Furthermore, most of these peptides have a highly hydrophobic N-terminus, similarly to the cluster 1 core sequence, which may serve as a hydrophobic anchor to facilitate stronger adsorption to the oil/water interface and high emulsion capacity. As Tryp and, to a lesser degree, Flav peptides also extend into this region compared to Neut peptides, this may be a key part of why Alc PPHs also show good emulsifying properties and why Flav PPHs perform better than Neut PPHs.

Although the contribution from cluster 4 peptides is smaller than cluster 1 and 3 peptides, it is noteworthy that a peptide (LADYFDVIGGTSTGGLLTAMITTPNENNRPFAAAK), corresponding to a slightly elongated version of γ36 (FDVIGGTSTGGLLTAMITTPNENNRP), was identified in all Tryp PPHs, exactly as predicted (Section 3.1). With increasing E/S ratio, the estimated abundance of this peptide also increased from 0.08% (I_{rel}) in 0.1% Tryp to 0.64% (I_{rel}) in 3% Tryp (Table A.4). This in spite of the total MS1 intensity more than doubled in 3% Tryp, indicating that increasing the DH towards completion for tryptic hydrolysis, substantially increases the release of the target peptide. This also correlates well with the high emulsifying and foaming properties observed for 3% Tryp PPH. The peptides were surprisingly also identified in all Alc and Flav PPHs, but at a substantially lower abundance ($I_{rel} < 0.05\%$). In Alc PPHs, several peptides of sufficient length for helical surface activity (>15 AAs) and covering the most of γ36, were identified at noteworthy I_{rel} (Table A.4). This is particularly the case in 3% Alc, where five peptides (16–34 AAs) were identified with $I_{rel} > 0.1\%$ (0.14–0.35%). In contrast, the most abundant cluster 4 peptides in e.g. 3% Neut (0.44–0.63%) were substantially shorter (12–16 AAs) and only covering the N-terminal part of the γ36 target sequence. This adds to the peptide-level evidence, substantiating why Tryp, but also Alc, PPHs have significantly higher emulsifying activity than Neut PPHs.

Peptide-centric analysis further indicates that mapping identified peptides onto a target cluster consensus sequence alone is not enough to describe high surface activity, but that a higher degree of peptide-level detail is needed. It also calls for further investigations to determine which parts of the target cluster sequences constitute the utmost important (core) region for functionality, thereby facilitating efficient peptide mapping that correlates with observed functionality. This may be addressed computationally through development of more sophisticated predictors, able to identify not only core regions but also other structural features of importance for emulsifying activity in addition to amphiphilicity, such as hydrophobic anchors. Moreover, estimating the abundance/concentration of a specific peptide merely by the MS1 intensity is a very rough and biased estimate, as intrinsic and sequence specific properties makes peptides behave and ionize differently in MS (Jarnuczak et al., 2016; Sinitcyn, Rudolph, & Cox, 2018). This highlights the need for fundamentally new computational approaches for absolute peptide quantification in highly complex mixtures such as hydrolysates, which is currently under investigation in our labs.

Interestingly, high intensity cluster 1 and 3 Alc peptides (Fig. 5 and Table A.3) indicate that Alc has strong preference to cleave after particularly Glu and Leu in both the N- and C-terminal. Similar trends were observed for high intensity cluster 4 Alc peptides (Table A.4). While Leu specificity was described by the manufacturer, Glu specificity was not. Nevertheless, this is in line with previous reports on Alc specificity (Doucet et al., 2003; Lu et al., 2021). These inconsistencies highlight a crucial aspect for successful application of the presented methodology. In addition to the need for core region mapping and accurate peptide abundance estimation, a high degree of insight on protease specificity is pivotal for making accurate *in silico* analysis and prediction of peptide release. This task is significantly easier to perform for highly specific proteases (e.g. trypsin), also highlighting the need for further development of high specificity industrial proteases, available in bulk amounts for cost-effective process design. Ultimately, these limitations do impose a barrier for developing a more holistic workflow that can accurately predict dynamic peptide release for a wide range of proteases as well as peptide functionality which, together, could serve as an integral part of the process design. Moreover, there is also need for further development in methodological aspects that can account for the entire peptide population and additive effects in order to accurately predict the bulk functionality of a hydrolysate. These aspects are also currently under investigation in our labs. In addition, process scalability is crucial for industrial relevance and should be investigated further in regards to peptidomic composition and functional properties.

3.6. *Protease and E/S ratio governs differential protein class selectivity in heat denatured PPI*

Using our previously published method for relative protein abundance estimation using length-normalized, relative MS1 intensity (Gregersen et al., 2021, 2022), it is possible to obtain insight on which proteins are abundantly represented in a hydrolysate and thereby also on protein-level enrichment and selectivity. By summing intensities for all peptides originating from the proteins, the potential peptide-level bias is alleviated to a large degree. This is the prerequire assumption used in the popular iBAQ approach for relative protein quantification (Schwanhüusser et al., 2011). Based on relative abundance by I_L^{rel}, protein-level abundances were pooled into major protein families/classes found in potato (Fig. 6, Table A.5). Compared to a previous study on the same PPI (García-Moreno, Gregersen, et al., 2020), patatin is enriched in Alc PPHs while somewhat depleted in Tryp PPHs. In fact, patatin represents more than double of the relative protein content in Alc PPHs (40–45%) compared to Tryp PPHs (18–19%) at 1% and 3% E/S ratio. The direct opposite is observed for Kunitz peptides, where Tryp PPHs at 1% and 3% E/S ratio contain twice the relative amount (46–54%) compared to Alc PPHs (23–25%). As both Alc and Tryp are serine endoproteases (Peyronel & Cantera, 1995), this is likely a direct result of different specificities. Consequently, Alc may be capable of hydrolysing patatin to a much higher degree prior to inhibition by Kunitz serine protease inhibitors (KTI-B class) which remain active to some extent despite heat treatment. This observation also correlates well with why the relative protein class distribution for Neut PPHs to a much higher extent reflects earlier MS-based proteomics studies of the PPI (García-Moreno, Gregersen, et al., 2020), as Neut is a Zinc-protease and limited inhibitory activity is expected in the PPI, as discussed in Section 3.2.

	Alcalase			Flavourzyme			Neutrase			Trypsin		
Class	0.1%	1%	3%	0.1%	1%	3%	0.1%	1%	3%	0.1%	1%	3%
Patatin	43.4%	45.1%	40.1%	31.4%	41.3%	36.4%	30.8%	27.6%	27.2%	31.6%	18.6%	18.4%
Kunitz_sum	25.8%	22.9%	24.6%	39.1%	25.2%	28.9%	41.1%	45.6%	48.0%	39.9%	50.3%	46.2%
KTI-A	0.2%	0.2%	0.3%	0.7%	0.3%	0.6%	1.2%	1.0%	0.7%	0.5%	0.9%	0.7%
KTI-B	14.0%	11.4%	11.3%	24.3%	14.8%	16.8%	15.9%	16.5%	16.7%	25.5%	21.6%	16.9%
KTI-C	2.3%	3.6%	4.9%	5.0%	3.0%	4.1%	11.8%	12.4%	12.4%	4.5%	15.0%	13.6%
KTI-D	2.3%	1.4%	1.5%	4.0%	2.7%	1.6%	1.7%	1.5%	1.5%	3.9%	2.0%	2.1%
Kunitz_unclassified	6.9%	6.4%	6.7%	5.2%	4.4%	5.8%	10.5%	14.3%	16.7%	5.5%	10.7%	12.9%
PIN	3.8%	5.6%	8.0%	5.7%	5.0%	6.8%	13.7%	12.4%	10.4%	5.9%	13.7%	14.0%
MCPI	0.2%	0.0%	0.0%	0.4%	0.2%	0.2%	0.1%	0.1%	0.1%	0.4%	0.4%	0.2%
Lipoxygenase	0.8%	0.8%	1.1%	0.8%	0.7%	0.7%	1.0%	1.2%	1.2%	0.8%	1.4%	1.9%
Other	25.9%	25.5%	26.2%	22.4%	27.4%	26.8%	13.4%	13.1%	13.1%	21.2%	15.2%	18.9%

	Alcalase			Flavourzyme			Neutrase			Trypsin		
Class	0.1%	1%	3%	0.1%	1%	3%	0.1%	1%	3%	0.1%	1%	3%
Patatin	43.4%	45.1%	40.1%	31.4%	41.3%	36.4%	30.8%	27.6%	27.2%	31.6%	18.6%	18.4%
Kunitz_sum	25.8%	22.9%	24.6%	39.1%	25.2%	28.9%	41.1%	45.6%	48.0%	39.9%	50.3%	46.2%
KTI-A	0.2%	0.2%	0.3%	0.7%	0.3%	0.6%	1.2%	1.0%	0.7%	0.5%	0.9%	0.7%
KTI-B	14.0%	11.4%	11.3%	24.3%	14.8%	16.8%	15.9%	16.5%	16.7%	25.5%	21.6%	16.9%
KTI-C	2.3%	3.6%	4.9%	5.0%	3.0%	4.1%	11.8%	12.4%	12.4%	4.5%	15.0%	13.6%
KTI-D	2.3%	1.4%	1.5%	4.0%	2.7%	1.6%	1.7%	1.5%	1.5%	3.9%	2.0%	2.1%
Kunitz_unclassified	6.9%	6.4%	6.7%	5.2%	4.4%	5.8%	10.5%	14.3%	16.7%	5.5%	10.7%	12.9%
PIN	3.8%	5.6%	8.0%	5.7%	5.0%	6.8%	13.7%	12.4%	10.4%	5.9%	13.7%	14.0%
MCPI	0.2%	0.0%	0.0%	0.4%	0.2%	0.2%	0.1%	0.1%	0.1%	0.4%	0.4%	0.2%
Lipoxygenase	0.8%	0.8%	1.1%	0.8%	0.7%	0.7%	1.0%	1.2%	1.2%	0.8%	1.4%	1.9%
Other	25.9%	25.5%	26.2%	22.4%	27.4%	26.8%	13.4%	13.1%	13.1%	21.2%	15.2%	18.9%

Fig. 6. Heat map (blue (low) to red (high)) of relative protein abundance (by unspecific I_L^{rel}) according to protein families/classes for all PPHs. Heat map color is normalized by row (top) and column (bottom) for inter- and intra-sample comparison, respectively. All indented Kunitz subclasses (A-D and unclassified) are included in the "Kunitz_sum" abundance, but are listed explicitly to distinguish quantitatively between subclasses. (For interpretation of the references to color in this figure legend, the reader is referred to the Web version of this article.)

For all subclasses of Kunitz-type inhibitors and the class proteinase inhibitors (PIN), substantial differences are observed across PPHs. This is of particular interest for the patatins, KTI-A, and KTI-B classes, as these represent all the target peptides (Table 1). As ten of the 15 target peptides originate from patatin isoforms, enrichment of patatin-derived peptides in Alc PPHs (Fig. 6) may be a direct reason for the strong emulsifying properties (Table 3), although Tryp PPH was both predicted to have substantially better emulsifying properties as well as shown to contain peptides with better overlap in the high abundance target clusters 1 and 3. This also illustrates potential for further improving the interfacial properties of Tryp PPHs even more, by improving hydrolysis conditions and obtaining a higher relative amount of patatin-derived peptides in the PPH. This may potentially be accomplished by combing enzymatic hydrolysis with other methods such as e.g. ultrasound and microwave treatment, previously shown to improve digestibility of potato protein (Cheng et al., 2017; Falade et al., 2021; Mao, Wu, Zhang, Ma, & Cheng, 2020). Nevertheless, our observations further substantiate how protease specificity and potential selectivity, search parameters, and hydrolysis conditions significantly affect the peptidome of a hydrolysate in differential manners. This is particularly relevant for short-term, partial enzymatic hydrolysis and also supported by differential observations for the class of "other" proteins (see supplementary for further elaboration).

4. Conclusion

In line with increasing focus on green transition and clean label foods, peptides and protein hydrolysates attract significant attention for substituting chemical additives as surface active ingredients in foods. With this work, we present a fundamentally novel workflow employing bioinformatics and data-driven process design for targeted hydrolysis, as an alternative to the conventional trial-and-error methodology. Using prior *in vitro* knowledge of highly potent emulsifier peptides derived from abundant potato proteins, we use *in silico* sequence analysis to hypothesize that Trypsin can release target peptides through hydrolysis and produce a hydrolysate with superior interfacial activity. This was verified through assessment of emulsifying and foaming properties and by benchmarking against the native substrate, a positive control (sodium caseinate), an enriched patatin fraction, and hydrolysates produced with a range of industrial proteases to different degrees of hydrolysis. In fact, only the application of Trypsin was able to improve both emulsification activity and stability significantly ($P < 0.05$) compared to untreated native substrate. Overall, we found a weak relation between degree of hydrolysis and bulk interfacial activity for the hydrolysates, but DH cannot by itself be used to assess emulsification potential. Using LC-MS/MS analysis, we were able to convert conventional bottom-up proteomics into a non-specific peptidomic analysis, identifying more than 10,000 peptides in each hydrolysate. Using peptide mapping, we show that random overlaps is insufficient for quantitatively describing bulk functionality of hydrolysates, but a deeper, peptide-centric analysis is required. Through this, we show that hydrolysates produced using Trypsin, and to some extent Alcalase, were rich in peptides with much higher amphiphilic potential than the other hydrolysates assayed. Moreover, the 3% tryptic hydrolysate was found

to contain predicted peptides, thereby not only validating our novel approach for targeted hydrolysis, but also providing peptide-level indications to why this particular hydrolysate had the best surface active properties across all hydrolysates investigated. Ultimately, based on modest yields, and that peptides from patatin appear depleted in the hydrolysate, we expect that optimizing process conditions will improve the surface active properties of the tryptic hydrolysate even further. This study further highlights several challenges and bottlenecks related to efficient, large-scale application of the methodology. For instance, a method for accurate and absolute peptide quantification is needed, and better characterization of protease specificity as well as a broader selection of high specificity industrial proteases are prerequisites for further development in this direction. Nevertheless, this study is yet another example of how interdisciplinary research, big data, and computational predictions is gaining headway in food science and can pave the way for more efficient development in the future while simultaneously providing a deeper fundamental understanding of molecular mechanisms and properties related to food ingredient functionality.

Author contribution

SGE: Conceptualization, Methodology, Formal analysis, Investigation, Validation, Writing – original draft preparation, Writing – review and editing, Visualization, Supervision. AJ: Methodology, Formal analysis, Investigation, Writing – original draft preparation, Writing – review and editing, Visualization. BY: Validation, Writing – review and editing. PJGM: Validation, Writing – review and editing. MGP: Methodology, Formal analysis, Writing – review and editing. DKH: Methodology, Formal analysis, Writing – review and editing. CJ: Conceptualization, Writing – review and editing, Funding acquisition, Supervision. MTO: Conceptualization, Methodology, Writing – review and editing, Funding acquisition, Supervision. EBH: Conceptualization, Writing – review and editing, Project administration, Funding acquisition, Supervision.

Funding

This work was supported by Innovation Fund Denmark (Grant number 7045-00021B (PROVIDE)).

Declaration of competing interest

The authors declare no conflict of interests.

Data availability

The mass spectrometry proteomics data have been deposited to the ProteomeXchange Consortium with the dataset identifier PXD034139. All other data will be mada available upon request.

Acknowledgements

The authors would like to acknowledge KMC AmbA for supplying the potato protein isolate and Lihme Protein Solutions (Denmark) for supplying purified patatin as a reference. Likewise, the authors would like to acknowledge Arla Foods A/S (Denmark) and Novozymes A/S (Denmark) for providing sodium caseinate and proteolytic enzymes, respectively.

Appendix A. Supplementary data

Supplementary data to this article can be found online at https://doi.org/10.1016/j.foodhyd.2022.108299.

References

Adjonu, R., Doran, G., Torley, P., & Agboola, S. (2014). Whey protein peptides as components of nanoemulsions: A review of emulsifying and biological functionalities. *Journal of Food Engineering, 122*, 15–27. https://doi.org/10.1016/j.jfoodeng.2013.08.034

Adler-Nissen, J. (1986). *Enzymatic hydrolysis of food proteins*. London: Elsevier Applied Science Publishers.

Akbari, N., Mohammadzadeh Milani, J., & Biparva, P. (2020). Functional and conformational properties of proteolytic enzyme-modified potato protein isolate. *Journal of the Science of Food and Agriculture, 100*(3), 1320–1327. https://doi.org/10.1002/jsfa.10148

Aldred, N., Phang, I. Y., Conlan, S. L., Clare, A. S., & Vancso, G. J. (2008). The effects of a serine protease, Alcalase, on the adhesives of barnacle cyprids (Balanus amphitrite). *Biofouling, 24*(2), 97–107. https://doi.org/10.1080/08927010801885908

Aluko, R. E. (2018). Food protein-derived peptides: Production, isolation, and purification. In *Proteins in food processing* (2nd ed., pp. 389–412). https://doi.org/10.1016/B978-0-08-100722-8.00016-4 Second Edi.

Ashaolu, T. J. (2020). Applications of soy protein hydrolysates in the emerging functional foods: A review. *International Journal of Food Science and Technology, 55*(2), 421–428. https://doi.org/10.1111/IJFS.14380

Avramenko, N. A., Low, N. H., & Nickerson, M. T. (2013). The effects of limited enzymatic hydrolysis on the physicochemical and emulsifying properties of a lentil protein isolate. *Food Research International, 51*(1), 162–169. https://doi.org/10.1016/J.FOODRES.2012.11.020

Barac, M., Cabrilo, S., Stanojevic, S., Pesic, M., Pavlicevic, M., Zlatkovic, B., et al. (2012). Functional properties of protein hydrolysates from pea (Pisum sativum, L) seeds. *International Journal of Food Science and Technology, 47*(7), 1457–1467. https://doi.org/10.1111/J.1365-2621.2012.02993.X

Bauw, G., Nielsen, H. V., Emmersen, J., Nielsen, K. L., Jørgensen, M., & Welinder, K. G. (2006). Patatins, Kunitz protease inhibitors and other major proteins in tuber of potato cv. *Kuras. FEBS Journal, 273*(15), 3569–3584. https://doi.org/10.1111/j.1742-4658.2006.05364.x

Bjornshave, A., Johansen, T. N., Amer, B., Dalsgaard, T. K., Holst, J. J., & Hermansen, K. (2019). Pre-meal and postprandial lipaemia in subjects with the metabolic syndrome: Effects of timing and protein quality (randomised crossover trial). *British Journal of Nutrition, 121*(3), 312–321. https://doi.org/10.1017/S0007114518003264

Camire, M. E., Kubow, S., & Donnelly, D. J. (2009). Potatoes and human health. *Critical Reviews in Food Science and Nutrition, 49*(10), 823–840. https://doi.org/10.1080/10408390903041996

Caron, J., Chataigné, G., Gimeno, J. P., Duhal, N., Goossens, J. F., Dhulster, P., et al. (2016). Food peptidomics of in vitro gastrointestinal digestions of partially purified bovine hemoglobin: Low-resolution versus high-resolution LC-MS/MS analyses. *Electrophoresis, 37*(13), 1814–1822. https://doi.org/10.1002/elps.201500559

Cheng, Y., Liu, Y., Wu, J., Ofori Donkor, P., Li, T., & Ma, H. (2017). Improving the enzymolysis efficiency of potato protein by simultaneous dual-frequency energy-gathered ultrasound pretreatment: Thermodynamics and kinetics. *Ultrasonics Sonochemistry, 37*, 351–359. https://doi.org/10.1016/j.ultsonch.2017.01.034

Chen, W., Liang, G., Li, X., He, Z., Zeng, M., Gao, D., et al. (2019). Effects of soy proteins and hydrolysates on fat globule coalescence and meltdown properties of ice cream. *Food Hydrocolloids, 94*, 279–286. https://doi.org/10.1016/J.FOODHYD.2019.02.045

Chuang, H.-L., Baskaran, R., Day, C. H., Lin, Y.-M., Ho, C.-C., Ho, T.-J., et al. (2020). Role of potato protein hydrolysate and exercise in preventing high-fat diet-induced hepatocyte apoptosis in senescence-accelerated mouse. *Journal of Food Biochemistry, 44*(12), Article e13525. https://doi.org/10.1111/JFBC.13525

Consortium, T. U., Bateman, A., Martin, M.-J., Orchard, S., Magrane, M., Agivetova, R., et al. (2021). UniProt: The universal protein knowledgebase in 2021. *Nucleic Acids Research, 49*(D1), D480–D489. https://doi.org/10.1093/NAR/GKAA1100

Cox, J., & Mann, M. (2008). MaxQuant enables high peptide identification rates, individualized p.p.b.-range mass accuracies and proteome-wide protein quantification. *Nature Biotechnology, 26*(12), 1367–1372. https://doi.org/10.1038/nbt.1511

Cui, Q., Sun, Y., Cheng, J., & Guo, M. (2022). Effect of two-step enzymatic hydrolysis on the antioxidant properties and proteomics of hydrolysates of milk protein concentrate. *Food Chemistry, 366*(July 2021), Article 130711. https://doi.org/10.1016/j.foodchem.2021.130711

Demirhan, E., Apar, D. K., & Özbek, B. (2011). Sesame cake protein hydrolysis by alcalase: Effects of process parameters on hydrolysis, solubilisation, and enzyme inactivation. *Korean Journal of Chemical Engineering, 28*(1), 195–202. https://doi.org/10.1007/s11814-010-0316-2

Deng, Y., van der Veer, F., Sforza, S., Gruppen, H., & Wierenga, P. A. (2018). Towards predicting protein hydrolysis by bovine trypsin. *Process Biochemistry, 65*, 81–92. https://doi.org/10.1016/J.PROCBIO.2017.11.006

Dexter, A. F. (2010). Interfacial and emulsifying properties of designed β-strand peptides. *Langmuir, 26*(23), 17997–18007. https://doi.org/10.1021/la103471j

Dexter, A. F., & Middelberg, A. P. J. (2008). Peptides as functional surfactants. *Industrial & Engineering Chemistry Research, 47*(17), 6391–6398. https://doi.org/10.1021/ie800127f

Donlon, J. (2007). Subtilisin. In J. Polaina, & A. P. MacCabe (Eds.), *Industrial enzymes; structure, function and applications* (pp. 197–206). Springer.

Doucet, D., Otter, D. E., Gauthier, S. F., & Foegeding, E. A. (2003). Enzyme-induced gelation of extensively hydrolyzed whey proteins by alcalase: Peptide identification and determination of enzyme specificity. *Journal of Agricultural and Food Chemistry, 51*(21), 6300–6308. https://doi.org/10.1021/jf026242v

Du, C., Cai, Y., Liu, T., Huang, L., Long, Z., Zhao, M., et al. (2020). Physicochemical, interfacial and emulsifying properties of insoluble soy peptide aggregate: Effect of homogenization and alkaline-treatment. *Food Hydrocolloids, 109*(June), Article 106125. https://doi.org/10.1016/j.foodhyd.2020.106125

Eisenberg, D., Weiss, R. M., & Terwilliger, T. C. (1982). The helical hydrophobic moment: A measure of the amphiphilicity of a helix. *Nature, 299*(5881), 371–374. https://doi.org/10.1038/299371a0

Elavarasan, K., Naveen Kumar, V., & Shamasundar, B. A. (2014). Antioxidant and functional properties of fish protein hydrolysates from fresh water carp (Catla catla) as influenced by the nature of enzyme. *Journal of Food Processing and Preservation, 38*(3), 1207–1214. https://doi.org/10.1111/jfpp.12081

Enser, M., Bloomberg, G. B., Brock, C., & Clark, D. C. (1990). De novo design and structure-activity relationships of peptide emulsifiers and foaming agents. *International Journal of Biological Macromolecules, 12*(2), 118–124. https://doi.org/10.1016/0141-8130(90)90063-G

Falade, E. O., Mu, T. H., & Zhang, M. (2021). Improvement of ultrasound microwave-assisted enzymatic production and high hydrostatic pressure on emulsifying, rheological and interfacial characteristics of sweet potato protein hydrolysates. *Food Hydrocolloids, 117*(February), Article 106684. https://doi.org/10.1016/j.foodhyd.2021.106684

Food and Agriculture Organization of the United Nations. (2020). *FAOSTAT statistical database*.

García Arteaga, V., Apéstegui Guardia, M., Muranyi, I., Eisner, P., & Schweiggert-Weisz, U. (2020). Effect of enzymatic hydrolysis on molecular weight distribution, techno-functional properties and sensory perception of pea protein isolates. *Innovative Food Science & Emerging Technologies, 65*, Article 102449. https://doi.org/10.1016/J.IFSET.2020.102449

García-Moreno, P. J., Gregersen, S., Nedamani, E. R., Olsen, T. H., Marcatili, P., Overgaard, M. T., et al. (2020). Identification of emulsifier potato peptides by bioinformatics: Application to omega-3 delivery emulsions and release from potato industry side streams. *Scientific Reports, 10*(1), 690. https://doi.org/10.1038/s41598-019-57229-6

García-Moreno, P. J., Jacobsen, C., Marcatili, P., Gregersen, S., Overgaard, M. T., Andersen, M. L., et al. (2020). Emulsifying peptides from potato protein predicted by bioinformatics: Stabilization of fish oil-in-water emulsions. *Food Hydrocolloids, 101*, Article 105529. https://doi.org/10.1016/j.foodhyd.2019.105529

García-Moreno, P. J., Yang, J., Gregersen, S., Jones, N. C., Berton-Carabin, C. C., Sagis, L. M. C., et al. (2021). The structure, viscoelasticity and charge of potato peptides adsorbed at the oil-water interface determine the physicochemical stability of fish oil-in-water emulsions. *Food Hydrocolloids, 115*, Article 106605. Retrieved from https://linkinghub.elsevier.com/retrieve/pii/S0268005X21000217.

Giansanti, P., Tsiatsiani, L., Low, T. Y., & Heck, A. J. R. (2016). Six alternative proteases for mass spectrometry-based proteomics beyond trypsin. *Nature Protocols, 11*(5), 993–1006. https://doi.org/10.1038/nprot.2016.057

Gregersen, S., Kongsted, A.-S. H., Nielsen, R. B., Hansen, S. S., Lau, F. A., Rasmussen, J. B., et al. (2021). Enzymatic extraction improves intracellular protein recovery from the industrial carrageenan seaweed Eucheuma denticulatum revealed by quantitative, subcellular protein profiling: A high potential source of functional food ingredients. *Food Chemistry X, 12*, Article 100137. https://doi.org/10.1016/J.FOCHX.2021.100137

Gregersen, S., Pertseva, M., Marcatili, P., Holdt, S. L., Jacobsen, C., Garcia-Moreno, P. J., et al. (2022). Proteomic characterization of pilot scale hot-water extracts from the industrial carrageenan red seaweed Eucheuma denticulatum. *Algal Research, 62*, Article 102619. https://doi.org/10.1016/J.ALGAL.2021.102619

Hanley, J., & James, T. (2018). Synthesis, chemistry, physicochemical properties and industrial applications of amino acid surfactants : A review. *Comptes Rendus Chimie*, 112–130. https://doi.org/10.1016/j.crci.2017.11.005

Hashemi, A., & Jafarpour, A. (2016). Rheological and microstructural properties of beef sausage batter formulated with fish fillet mince. *Journal of Food Science & Technology, 53*(1), 601–610. https://doi.org/10.1007/s13197-015-2052-4

Heibges, A., Glaczinski, H., Ballvora, A., Salamini, F., & Gebhardt, C. (2003). Structural diversity and organization of three gene families for Kunitz-type enzyme inhibitors from potato tubers (Solanum tuberosum l.). *Molecular Genetics and Genomics, 269*(4), 526–534. https://doi.org/10.1007/s00438-003-0860-0

Hinnenkamp, C., & Ismail, B. P. (2021). A proteomics approach to characterizing limited hydrolysis of whey protein concentrate. *Food Chemistry, 350*(February), Article 129235. https://doi.org/10.1016/j.foodchem.2021.129235

Huang, Y. P., Dias, F. F. G., Leite Nobrega de Moura Bell, J. M., & Barile, D. (2022). A complete workflow for discovering small bioactive peptides in foods by LC-MS/MS: A case study on almonds. *Food Chemistry, 369*, Article 130834. https://doi.org/10.1016/j.foodchem.2021.130834

Huang, D. Y., Swanson, B. G., & Ryan, C. A. (1981). Stability of proteinase inhibitors in potato tubers during cooking. *Journal of Food Science, 46*(1), 287–290. https://doi.org/10.1111/j.1365-2621.1981.tb14583.x

Jafarpour, A., Gomes, R. M., Gregersen, S., Sloth, J. J., Jacobsen, C., & Moltke Sørensen, A. D. (2020). Characterization of cod (Gadus morhua) frame composition and its valorization by enzymatic hydrolysis. *Journal of Food Composition and Analysis, 89*, Article 103469. https://doi.org/10.1016/j.jfca.2020.103469

Jafarpour, A., Gregersen, S., Marciel Gomes, R., Marcatili, P., Hegelund Olsen, T., Jacobsen, C., et al. (2020). Biofunctionality of enzymatically derived peptides from Codfish (Gadus morhua) frame: Bulk in vitro properties, quantitative proteomics, and bioinformatic prediction. *Marine Drugs, 18*(12), 599. https://doi.org/10.3390/md18120599

Jarnuczak, A. F., Lee, D. C. H., Lawless, C., Holman, S. W., Eyers, C. E., & Hubbard, S. J. (2016). Analysis of intrinsic peptide detectability via integrated label-free and SRM-based absolute quantitative proteomics. *Journal of Proteome Research, 15*(9), 2945–2959. https://doi.org/10.1021/acs.jproteome.6b00048

Jin, Y., Yan, J., Yu, Y., & Qi, Y. (2015). Screening and identification of DPP-IV inhibitory peptides from deer skin hydrolysates by an integrated approach of LC-MS/MS and in silico analysis. *Journal of Functional Foods, 18*, 344–357. https://doi.org/10.1016/j.jff.2015.07.015

Jones, D. B. (1931). *Factors for converting percentages of nitrogen in foods and feeds into percentages of protein*.

Jørgensen, M., Bauw, G., & Welinder, K. G. (2006). Molecular properties and activities of tuber proteins from starch potato cv. *Kuras. Journal of Agricultural and Food Chemistry, 54*(25), 9389–9397. https://doi.org/10.1021/jf0623945

Jørgensen, M., Stensballe, A., & Welinder, K. G. (2011). Extensive post-translational processing of potato tuber storage proteins and vacuolar targeting. *FEBS Journal, 278*(21), 4070–4087. https://doi.org/10.1111/j.1742-4658.2011.08311.x

Kamnerdpetch, C., Weiss, M., Kasper, C., & Scheper, T. (2007). An improvement of potato pulp protein hydrolyzation process by the combination of protease enzyme systems. *Enzyme and Microbial Technology, 40*(4), 508–514. https://doi.org/10.1016/j.enzmictec.2006.05.006

Karami, Z., & Akbari-adergani, B. (2019). Bioactive food derived peptides: A review on correlation between structure of bioactive peptides and their functional properties. *Journal of Food Science & Technology, 56*(2), 535–547. https://doi.org/10.1007/s13197-018-3549-4

Kärenlampi, S. O., & White, P. J. (2009). Potato proteins, lipids, and minerals. In *Advances in potato chemistry and technology* (pp. 99–125). https://doi.org/10.1016/b978-0-12-374349-7.00005-2

Klompong, V., Benjakul, S., Kantachote, D., & Shahidi, F. (2007). Antioxidative activity and functional properties of protein hydrolysate of yellow stripe trevally (Selaroides leptolepis) as influenced by the degree of hydrolysis and enzyme type. *Food Chemistry, 102*(4), 1317–1327. https://doi.org/10.1016/j.foodchem.2006.07.016

Lacou, L., Léonil, J., & Gagnaire, V. (2016). June 1). Functional properties of peptides: From single peptide solutions to a mixture of peptides in food products. *Food Hydrocolloids, 57*, 187–199. https://doi.org/10.1016/j.foodhyd.2016.01.028

Le Guenic, S., Chaveriat, L., Lequart, V., Joly, N., & Martin, P. (2019). Renewable surfactants for biochemical applications and nanotechnology. *Journal of Surfactants and Detergents, 22*(1), 5–21. https://doi.org/10.1002/jsde.12216

Lei, F., Cui, C., Zhao, Q., Sun-Waterhouse, D., & Zhao, M. (2014). Evaluation of the hydrolysis specificity of protease from marine Exiguobacterium sp. SWJS2 via free amino acid analysis. *Applied Biochemistry and Biotechnology, 174*(4), 1260–1271. https://doi.org/10.1007/s12010-014-1088-7

Li-Chan, E. C. Y. (2015). February 1). Bioactive peptides and protein hydrolysates: Research trends and challenges for application as nutraceuticals and functional food ingredients. *Current Opinion in Food Science, 1*, 28–37. https://doi.org/10.1016/j.cofs.2014.09.005

Liang, G., Chen, W., Qie, X., Zeng, M., Qin, F., He, Z., et al. (2020). Modification of soy protein isolates using combined pre-heat treatment and controlled enzymatic hydrolysis for improving foaming properties. *Food Hydrocolloids, 105*(May 2019), Article 105764. https://doi.org/10.1016/j.foodhyd.2020.105764

Li, X., Deng, J., Shen, S., Li, T., Yuan, M., Yang, R., et al. (2015). Antioxidant activities and functional properties of enzymatic protein hydrolysates from defatted Camellia oleifera seed cake. *Journal of Food Science & Technology, 52*(9), 5681–5690. https://doi.org/10.1007/s13197-014-1693-z

Linderstrøm-Lang, K. (1953). The initial phases of the enzymatic degradation of proteins. *Bulletin de la Societe de Chimie Biologique, 35*(1–2), 100–116.

Liu, Q., Kong, B., Xiong, Y. L., & Xia, X. (2010). Antioxidant activity and functional properties of porcine plasma protein hydrolysate as influenced by the degree of hydrolysis. *Food Chemistry, 118*(2), 403–410. https://doi.org/10.1016/j.foodchem.2009.05.013

Liu, Z., Su, Y., & Zeng, M. (2011). Amino acid composition and functional properties of giant red sea cucumber (Parastichopus californicus) collagen hydrolysates. *Journal of Ocean University of China, 10*(1), 80–84. https://doi.org/10.1007/S11802-011-1787-4, 2011 10:1.

Li, M., Zheng, H., Lin, M., Zhu, W., & Zhang, J. (2020). Characterization of the protein and peptide of excipient zein by the multi-enzyme digestion coupled with nano-LC-MS/MS. *Food Chemistry, 321*(October 2019), Article 126712. https://doi.org/10.1016/j.foodchem.2020.126712

Løkra, S., & Strætkvern, K. O. (2009). Industrial proteins from potato juice. A review. *Food, 3*(1), 88–95.

Lu, X., Sun, Q., Zhang, L., Wang, R., Gao, J., Jia, C., et al. (2021). Dual-enzyme hydrolysis for preparation of ACE-inhibitory peptides from sesame seed protein: Optimization, separation, and identification. *Journal of Food Biochemistry, 45*(4), 1–18. https://doi.org/10.1111/jfbc.13638

Mao, C., Wu, J., Zhang, X., Ma, F., & Cheng, Y. (2020). Improving the solubility and digestibility of potato protein with an online ultrasound-assisted PH shifting treatment at medium temperature. *Foods, 9*(12), 1908. https://doi.org/10.3390/FOODS9121908, 2020, Vol. 9, Page 1908.

Mariotti, F., Tomé, D., & Mirand, P. P. (2008). Converting nitrogen into protein—beyond 6.25 and jones' factors. *Critical Reviews in Food Science and Nutrition, 48*(2), 177–184. https://doi.org/10.1080/10408390701279749

McClements, D. J., & Jafari, S. M. (2018). Improving emulsion formation, stability and performance using mixed emulsifiers: A review. *Advances in Colloid and Interface Science, 251*, 55–79. https://doi.org/10.1016/j.cis.2017.12.001

Miedzianka, J., Pęksa, A., Pokora, M., Rytel, E., Tajner-Czopek, A., & Kita, A. (2014). Improving the properties of fodder potato protein concentrate by enzymatic hydrolysis. *Food Chemistry, 159*, 512–518. https://doi.org/10.1016/j.foodchem.2014.03.054

Mokni Ghribi, A., Maklouf Gafsi, I., Sila, A., Blecker, C., Danthine, S., Attia, H., et al. (2015). Effects of enzymatic hydrolysis on conformational and functional properties of chickpea protein isolate. *Food Chemistry, 187*, 322–330. https://doi.org/10.1016/J.FOODCHEM.2015.04.109

Mondal, S., Varenik, M., Bloch, D. N., Atsmon-Raz, Y., Jacoby, G., Adler-Abramovich, L., et al. (2017). A minimal length rigid helical peptide motif allows rational design of modular surfactants. *Nature Communications, 8*. https://doi.org/10.1038/ncomms14018

Morales-Medina, R., Tamm, F., Guadix, A. M., Guadix, E. M., & Drusch, S. (2016). Functional and antioxidant properties of hydrolysates of sardine (S. pilchardus) and horse mackerel (T. mediterraneus) for the microencapsulation of fish oil by spray-drying. *Food Chemistry, 194*, 1208–1216. https://doi.org/10.1016/J.FOODCHEM.2015.08.122

Moreno, M. C. M., Cuadrado, V. F., Marquez Moreno, M. C., & Fernandez Cuadrado, V. (1993). Enzymic hydrolysis of vegetable proteins: Mechanism and kinetics. *Process Biochemistry, 28*(7), 481–490. https://doi.org/10.1016/0032-9592(93)85032-B

Nakai, S., Alizadeh-Pasdar, N., Dou, J., Buttimor, R., Rousseau, D., & Paulson, A. (2004). Pattern similarity analysis of amino acid sequences for peptide emulsification. *Journal of Agricultural and Food Chemistry, 52*(4), 927–934. https://doi.org/10.1021/jf034744i

Nisov, A., Ercili-Cura, D., & Nordlund, E. (2020). Limited hydrolysis of rice endosperm protein for improved techno-functional properties. *Food Chemistry, 302*(February 2019), Article 125274. https://doi.org/10.1016/j.foodchem.2019.125274

Nongonierma, A. B., Paolella, S., Mudgil, P., Maqsood, S., & FitzGerald, R. J. (2017). Dipeptidyl peptidase IV (DPP-IV) inhibitory properties of camel milk protein hydrolysates generated with trypsin. *Journal of Functional Foods, 34*, 49–58. https://doi.org/10.1016/j.jff.2017.04.016

O'Keeffe, M. B., & FitzGerald, R. J. (2014). Antioxidant effects of enzymatic hydrolysates of whey protein concentrate on cultured human endothelial cells. *International Dairy Journal, 36*(2), 128–135. https://doi.org/10.1016/j.idairyj.2014.01.013

Padial-Domínguez, M., Espejo-Carpio, F. J., Pérez-Gálvez, R., Guadix, A., & Guadix, E. M. (2020). Optimization of the emulsifying properties of food protein hydrolysates for the production of fish oil-in-water emulsions. *Foods, 9*(5), 636. https://doi.org/10.3390/foods9050636

Pearce, K. N., & Kinsella, J. E. (1978). Emulsifying properties of proteins: Evaluation of a turbidimetric technique. *Journal of Agricultural and Food Chemistry, 26*(3), 716–723. https://doi.org/10.1021/jf60217a041

Pęksa, A., & Miedzianka, J. (2014). Amino acid composition of enzymatically hydrolysed potato protein preparations. *Czech Journal of Food Sciences, 32*(3), 265–272. https://doi.org/10.17221/286/2013-cjfs

Pęksa, A., & Miedzianka, J. (2021). Potato industry by-products as a source of protein with beneficial nutritional, functional, health-promoting and antimicrobial properties. *Applied Sciences, 11*(8). https://doi.org/10.3390/app11083497

Perez-Riverol, Y., Bai, J., Bandla, C., García-Seisdedos, D., Hewapathirana, S., Kamatchinathan, S., et al. (2022). The PRIDE database resources in 2022: A hub for mass spectrometry-based proteomics evidences. *Nucleic Acids Research, 50*(D1), D543–D552. https://doi.org/10.1093/NAR/GKAB1038

Peyronel, D. V., & Cantera, A. M. B. (1995). A simple and rapid technique for postelectrophoretic detection of proteases using azocasein. *Electrophoresis, 16*(1), 1894–1897. https://doi.org/10.1002/elps.11501601311

Pouvreau, L., Gruppen, H., Piersma, S. R. R., van den Broek, L. A. A. M., Van Koningsveld, G. A. A., & Voragen, A. G. J. (2001). Relative abundance and inhibitory distribution of protease inhibitors in potato juice from cv. Elkana. *Journal of Agricultural and Food Chemistry, 49*(6), 2864–2874. https://doi.org/10.1021/jf010126v

Rabe, S., Fischer, L., Blank, I., Berends, P., Appel, D., Eisele, T., et al. (2015). Flavourzyme, an enzyme preparation with industrial relevance: Automated nine-step purification and partial characterization of Eight enzymes. *Journal of Agricultural and Food Chemistry, 63*(23), 5682–5693. https://doi.org/10.1021/acs.jafc.5b01665

Ralet, M. C., & Guéguen, J. (2000). Fractionation of potato proteins: Solubility, thermal coagulation and emulsifying properties. *LWT - Food Science and Technology, 33*(5), 380–387. https://doi.org/10.1006/fstl.2000.0672

Refstie, S., & Tiekstra, H. A. J. (2003). Potato protein concentrate with low content of solanidine glycoalkaloids in diets for Atlantic salmon (Salmo salar). *Aquaculture, 216*(1–4), 283–298. https://doi.org/10.1016/S0044-8486(02)00434-9

Ricardo, F., Pradilla, D., Cruz, J. C., & Alvarez, O. (2021). Emerging emulsifiers: Conceptual basis for the identification and rational design of peptides with surface activity. *International Journal of Molecular Sciences, 22*(9), 4615. https://doi.org/10.3390/ijms22094615

Rodan, K., Fields, K., & Falla, T. (2013). Bioactive peptides. *Cosmeceuticals and Cosmetic Practice*, 142–152. https://doi.org/10.1002/9781118384824.ch14

Ruiz-Álvarez, J. M., del Castillo-Santaella, T., Maldonado-Valderrama, J., Guadix, A., Guadix, E. M., & García-Moreno, P. J. (2022). pH influences the interfacial properties of blue whiting (M. poutassou) and whey protein hydrolysates determining the physical stability of fish oil-in-water emulsions. *Food Hydrocolloids, 122*, Article 107075. https://doi.org/10.1016/J.FOODHYD.2021.107075

Saito, M., Ogasawara, M., Chikuni, K., & Shimizu, M. (1995). Synthesis of a peptide emulsifier with an amphiphilic structure. *Bioscience Biotechnology and Biochemistry, 59*(3), 388–392. https://doi.org/10.1271/bbb.59.388

Sbroggio, M. F., Montilha, M. S., Figueiredo, V. R. G. de, Georgetti, S. R., & Kurozawa, L. E. (2016). Influence of the degree of hydrolysis and type of enzyme on antioxidant activity of okara protein hydrolysates. *Food Science and Technology, 36*(2), 375–381. https://doi.org/10.1590/1678-457X.000216

Schmidt, J. M., Damgaard, H., Greve-Poulsen, M., Sunds, A. V., Larsen, L. B., & Hammershøj, M. (2019). Gel properties of potato protein and the isolated fractions of patatins and protease inhibitors – impact of drying method, protein concentration, pH and ionic strength. *Food Hydrocolloids, 96*, 246–258. https://doi.org/10.1016/j.foodhyd.2019.05.022

Schwanhüusser, B., Busse, D., Li, N., Dittmar, G., Schuchhardt, J., Wolf, J., et al. (2011). Global quantification of mammalian gene expression control. *Nature, 473*(7347), 337–342. https://doi.org/10.1038/nature10098

Siebert, K. J. (2001). Quantitative structure-activity relationship modeling of peptide and protein behavior as a function of amino acid composition. *Journal of Agricultural and Food Chemistry, 49*(2), 851–858. https://doi.org/10.1021/jf000718y

Sinitcyn, P., Rudolph, J. D., & Cox, J. (2018). Computational methods for understanding mass spectrometry–based shotgun proteomics data. *Annual Review of Biomedical Data Science, 1*(1), 207–234. https://doi.org/10.1146/annurev-biodatasci-080917-013516

Taherian, A. R., Britten, M., Sabik, H., & Fustier, P. (2011). Ability of whey protein isolate and/or fish gelatin to inhibit physical separation and lipid oxidation in fish oil-in-water beverage emulsion. *Food Hydrocolloids, 25*(5), 868–878. https://doi.org/10.1016/j.foodhyd.2010.08.007

Tamm, F., Gies, K., Diekmann, S., Serfert, Y., Strunskus, T., Brodkorb, A., et al. (2015). Whey protein hydrolysates reduce autoxidation in microencapsulated long chain polyunsaturated fatty acids. *European Journal of Lipid Science and Technology, 117*(12), 1960–1970. https://doi.org/10.1002/ejlt.201400574

Tyanova, S., Temu, T., & Cox, J. (2016). The MaxQuant computational platform for mass spectrometry-based shotgun proteomics. *Nature Protocols, 11*(12), 2301–2319. https://doi.org/10.1038/nprot.2016.136

Van Koningsveld, G. A., Gruppen, H., De Jongh, H. H. J., Wijngaards, G., Van Boekel, M. A. J. S., Walstra, P., et al. (2001). Effects of pH and heat treatments on the structure and solubility of potato proteins in different preparations. *Journal of Agricultural and Food Chemistry, 49*(10), 4889–4897. https://doi.org/10.1021/jf010340j

Van Koningsveld, G. A., Walstra, P., Voragen, A. G. J. J., Kuijpers, I. J., Van Boekel, M. A., & Gruppen, H. (2006). Effects of protein composition and enzymatic activity on formation and properties of potato protein stabilized emulsions. *Journal of Agricultural and Food Chemistry, 54*(17), 6419–6427. https://doi.org/10.1021/jf061278z

Vioque, J., Sánchez-vioque, R., Clemente, A., Pedroche, J., & Millán, F. (2000). Partially hydrolyzed rapeseed protein isolates with improved functional properties. *Water*, (4), 447–450. https://doi.org/10.1007/s11746-000-0072-y

Waglay, A., & Karboune, S. (2016a). Enzymatic generation of peptides from potato proteins by selected proteases and characterization of their structural properties. *Biotechnology Progress, 32*(2), 420–429. https://doi.org/10.1002/btpr.2245

Waglay, A., & Karboune, S. (2016b). Potato proteins: Functional food ingredients. In *Advances in potato chemistry and technology* (2nd ed., pp. 75–104). Second Edi. https://doi.org/10.1016/B978-0-12-800002-1.00004-2.

Wang, L. L., & Xiong, Y. L. (2005). Inhibition of lipid oxidation in cooked beef patties by hydrolyzed potato protein is related to its reducing and radical scavenging ability. *Journal of Agricultural and Food Chemistry, 53*(23). https://doi.org/10.1021/jf051213g

Wouters, A. G. B., Rombouts, I., Fierens, E., Brijs, K., & Delcour, J. A. (2016). Relevance of the functional properties of enzymatic plant protein hydrolysates in food systems. *Comprehensive Reviews in Food Science and Food Safety, 15*(4), 786–800. https://doi.org/10.1111/1541-4337.12209

Wu, J. W., & Chen, X. L. (2011). Extracellular metalloproteases from bacteria. *Applied Microbiology and Biotechnology, 92*(2), 253–262. https://doi.org/10.1007/s00253-011-3532-8

Wu, Y.-H., Samuel, C., Chen, Y.-, Wu, Y.-H. S., & Chen, Y.-C. (2022). Trends and applications of food protein-origin hydrolysates and bioactive peptides. *Journal of Food and Drug Analysis, 30*(2), 172–184. https://doi.org/10.38212/2224-6614.3408

Wychowaniec, J. K., Patel, R., Leach, J., Mathomes, R., Chhabria, V., Patil-Sen, Y., et al. (2020). Aromatic stacking facilitated self-assembly of ultrashort ionic Complementary peptide sequence: β-Sheet nanofibers with remarkable gelation and interfacial properties. *Biomacromolecules, 21*(7), 2670–2680. https://doi.org/10.1021/acs.biomac.0c00366

Yesiltas, B., Gregersen, S., Lægsgaard, L., Brinch, M. L., Olsen, T. H., Marcatili, P., et al. (2021). Emulsifier peptides derived from seaweed, methanotrophic bacteria, and potato proteins identified by quantitative proteomics and bioinformatics. *Food Chemistry, 362*, Article 130217. https://doi.org/10.1016/J.FOODCHEM.2021.130217

Yu, C., Zheng, L., Cai, Y., Zhao, Q., & Zhao, M. (2022). Desirable characteristics of casein peptides with simultaneously enhanced emulsion forming ability and antioxidative capacity in O/W emulsion. *Food Hydrocolloids, 131*, Article 107812. https://doi.org/10.1016/J.FOODHYD.2022.107812

Zhao, X., & Hou, Y. (2009). Limited hydrolysis of soybean protein concentrate and isolate with two proteases and the impact on emulsifying activity index of hydrolysates. *African Journal of Biotechnology, 8*(14), 3314–3319. https://doi.org/10.5897/AJB09.262

Zhao, Q., Xiong, H., Selomulya, C., Chen, X. D., Zhong, H., Wang, S., et al. (2012). Enzymatic hydrolysis of rice dreg protein: Effects of enzyme type on the functional properties and antioxidant activities of recovered proteins. *Food Chemistry, 134*(3), 1360–1367. https://doi.org/10.1016/j.foodchem.2012.03.033